Wheat *EARLY FLOWERING3* is a dawn-expressed circadian oscillator component that regulates heading date

Lukas Wittern[1¶], Gareth Steed[1¶], Laura J. Taylor[1], Dora Cano Ramirez[1], Gabriela Pingarron-Cardenas,[1] Keith Gardner[2], Andy Greenland[2], Matthew A. Hannah[3], Alex A. R. Webb[1*]

[1] Department of Plant Sciences, University of Cambridge, Downing Street, Cambridge, CB2 3EA, UK

[2] NIAB, Huntingdon Road, Cambridge, UK

[3] BASF, BBCC – Innovation Center Gent, Technologiepark-Zwijnaarde, Gent, Belgium

*Corresponding author

Email: aarw2@cam.ac.uk (AARW)

¶These authors contributed equally to this work

Abstract

Using an eight-parent Multiparent Advanced Generation Inter-Cross (MAGIC) population we investigated how variation at circadian clock-associated genes contributes to the regulation of heading date in UK and European winter wheat varieties. We identified homoeologues of *EARLY FLOWERING* 3 (*ELF3*) as candidates for the *Earliness per se* (*Eps*) *D1* and *B1 loci* in field conditions. We confirmed that a SNP within the coding region of *TaELF3-B1* is a candidate polymorphism underlying the *Eps-B1 locus.* We found that a reported deletion at the *Eps-D1 locus* encompassing *TaELF3-D1,* is instead a novel allele that lies within an introgression region containing an inversion relative to the Chinese Spring D genome. Using *T. turgidum cv. Kronos* carrying loss of function alleles of *TtELF3* we show that *ELF3* does regulate heading by demonstrating that the loss of a single *ELF3* homoeologue was sufficient to alter heading date. These studies demonstrated that *ELF3* forms part of the circadian oscillator but loss of all homoeologues was required to affect circadian rhythms. Similarly, loss of functional *LUX ARRHYTHMO* (*LUX*) in *T. aestivum*, an orthologue of a protein partner of Arabidopsis ELF3, severely disrupted circadian rhythms. *ELF3* and *LUX* transcripts are not co-expressed at dusk suggesting the structure of the wheat circadian oscillator might differ to that of Arabidopsis. Our demonstration that alteration to *ELF3* homoeologues can affect heading date separate from effects on the circadian oscillator suggests a role for *ELF3* in cereal photoperiodic responses that could be selected for, without pleiotropic deleterious alterations to circadian rhythms.

53 # Introduction

54 Circadian clocks are endogenous timing mechanisms with a near 24 hour period that
55 sequence biological events, provide anticipation of environmental rhythms and permit
56 measurement of daylength to regulate seasonal adjustments (McClung 2019). Plant
57 breeders have indirectly selected for variation at circadian-associated *loci* in many of
58 the world's major crops when breeding to increase yield and improve crop
59 performance by adapting genotypes to the local environment (Steed et al. 2021). Here
60 we investigated whether variation at circadian-associated *loci* contributes to wheat
61 yield traits in the field using a Multiparent Advanced Generation Inter-Cross (MAGIC)
62 mapping population (Mackay *et al.* 2014). Wheat is a major crop, providing
63 approximately 20% of the dietary calories and protein for the world's population
64 (Hawkesford *et al.* 2013). Since the green revolution wheat yields have continued to
65 increase but with the world's population estimated to reach 9.6 billion in 2050 (Gerland
66 *et al.* 2014) it is likely that demand will outpace predicted yield increases (Hawkesford
67 *et al.* 2013). Identification of novel genetic variation contributing to yield is critical to
68 increasing the rate of yield gains in wheat.
69
70 Understanding of the nature of plant circadian oscillators is based primarily on
71 investigation of Arabidopsis. In that model, the circadian oscillator contains a series of
72 interlocking transcriptional feedback loops. The circadian oscillator cycle can be
73 considered to start at dawn when expression of the transcriptional repressors
74 *CIRCADIAN CLOCK ASSOCIATED 1* (*CCA1*) and *LATE ELONGATED HYPOCOTYL*
75 (*LHY*) peaks, followed sequentially by peaks of expression of *PSEUDO RESPONSE*
76 *REGULATOR 9* (*PRR9*), *PRR7, PRR5, PRR3* and finally *PRR1* (also known as
77 *TIMING OF CAB EXPRESSION 1* (*TOC1*)) at dusk (Hsu and Harmer 2014). PRR9

78 and PRR7 repress the expression of *CCA1* and *LHY* which releases repression of
79 evening phased genes including, *TOC1, GIGANTEA* (*GI*)*, EARLY FLOWERING 3*
80 (*ELF3*)*, ELF4* and *LUX ARRHYTHMO* (*LUX*) (Hsu and Harmer 2014). LUX is a MYB-
81 like transcription factor which associates with ELF3 and ELF4 to form the tripartite
82 evening complex (EC), which represses expression of *GI, TOC1, PRR7, PRR9* and
83 *LUX* (Dixon *et al.* 2011, Nusinow *et al.* 2011, Herrero *et al.* 2012). Mutation of any of
84 the three EC components causes arrhythmia of the Arabidopsis circadian oscillator in
85 continuous light and temperature (Nagel and Kay 2012).
86
87 Orthologues of *ELF3* underlie *loci* regulating heading date in multiple crops, including
88 barley *early maturity8* (*eam8*) (Faure *et al.* 2012), rice *heading date17* (*Hd17*)
89 (Matsubara *et al.* 2012), *Earliness per se* (*Eps*)-A^{m}*1* in *T. monococcum* and *Eps-D1* in
90 *T. aestivum* (Zikhali *et al.* 2016). In hexaploid wheat, the magnitude of the *Eps-D1*
91 effect on heading date increases with decreasing temperature (Ochagavía *et al.* 2019).
92 Orthologues of *TOC1* are associated with heading date, plant height and thousand
93 grain weight (Sun *et al.* 2020). An orthologue of *LUX* is a candidate for *Eps-3*A^{m} in *T.*
94 *monococcum* (Gawronski *et al.* 2014) and *HvLUX* is a candidate gene for *eam10* in
95 barley (Campoli *et al.* 2013). Furthermore, the *Photoperiod-1* (*Ppd-1*) genes, which
96 contribute to photoperiodic regulation of ear emergence, are orthologues of
97 Arabidopsis *PRRs* (Beales *et al.* 2007, Shaw *et al.* 2012, Bentley *et al.* 2013, Turner
98 *et al.* 2013).
99
100 We used the allelic diversity of a wheat MAGIC population to investigate the role of
101 circadian clock genes in regulating yield component traits in the field. The parent
102 varieties for the MAGIC population used in this study (Alchemy, Brompton, Claire,
103 Hereward, Rialto, Robigus, Soissons and Xi-19) are representative of UK and

104 European winter wheat varieties, capturing >80% of the polymorphism found across
105 UK wheat varieties from the last 70 years (Gardner *et al.* 2016). Our data demonstrate
106 that modified *ELF3* function can affect the regulation of flowering time without
107 disrupting circadian oscillations and thus potentially avoid associated yield penalties
108 (Dodd *et al.* 2005). Together, this suggests *ELF3* is a possible breeding target for crop
109 improvement. We find evidence that in wheat *ELF3* is expressed in the morning, rather
110 than the evening as it is in Arabidopsis and conclude there are likely differences in the
111 role for *ELF3* in the circadian system between wheat and Arabidopsis. Our finding of
112 separable roles for *ELF3* in the circadian oscillator and the regulation of heading date
113 suggest a direct role for ELF3 in photoperiodic regulation in cereals.
114

115 Results

116 Earliness per se *loci Eps-B1* and *Eps-D1* segregate in an 117 eight-parent wheat MAGIC population

118 We performed QTL analysis on a set of replicated trial data for 784 recombinant inbred
119 lines (RILs) for the NIAB Elite MAGIC population from the 2012/2013 and 2013/2014
120 growing seasons at the NIAB experimental farms in Cambridge, UK. Growth stage 55
121 (GS55, equivalent to heading date) (Zadoks *et al.* 1974) was chosen for analysis and
122 QTL mapping to enable comparisons with previous studies (Griffiths *et al.* 2009). In
123 both 2013 and 2014, Soissons, which contains the *Ppd-D1a* (photoperiod insensitive)
124 allele, reached GS55 6-8 days earlier than any of the other MAGIC parents, which
125 contain the *Ppd-D1b* allele (photoperiod sensitive) (Figure 1). Heading date of the
126 other MAGIC parents varied over 5.5 days in 2013 and 7 days in 2014.
127

128 We performed the QTL analysis using MPWGAIM (Verbyla *et al.* 2014) for GS55
129 phenotypes in both years and tested whether any circadian clock genes co-locate
130 with the identified QTLs (< 2 cM to nearest 90 k marker or < 5 Mb to gene). Because
131 we are interested in the effects of the circadian clock on yield traits, we report only
132 QTLs associated with circadian clock genes. We found that four circadian gene
133 orthologues (*TaELF3-B1, TaELF3-D1, Ppd-1, TaZTL-7A*) fell within 0.20, 0.27, 0.58
134 and 4.31 Mb respectively of one of the QTL flanking markers (Table 1). The absence
135 of significant heading date QTLs linked to vernalisation genes such as *VRN1*
136 confirmed that complete vernalisation had occurred, ensuring that observed
137 variations in heading date were true *Earliness per-se* (*Eps*) effects rather than a
138 variation in the vernalisation requirements between the MAGIC parents (Bentley *et*
139 *al.* 2013, Camargo *et al.* 2016). A previous study identified a single GS55 QTL in the
140 NIAB eight-parent MAGIC population (Camargo *et al.* 2016) but this difference in
141 findings is likely a result of different growth conditions (greenhouse compared to
142 field), lower replicate number (208 RILs in pots compared to 784 RILs in field plots)
143 and the use of a different mapping methodology. Further validation of our analysis
144 pipeline and approaches are described in the methods and reported in
145 (Supplemental Table S1).
146
147 A QTL on the distal end of chromosome 1B, delineated by the markers
148 Ra_c109187_371 and RAC875_c37075_283, mapped closely to the physical position
149 of *TaELF3-B1* (TraesCS1B02G477400) (Table 1). The 1B locus also had a
150 homoeologous QTL on chromosome 1D delineated by the markers Kukri_c29687_369
151 and Kukri_rep_c69829_307 identifying *TaELF3-D1* (TraesCS1D02G451200) as a
152 candidate gene (Table 1, Figure 2A). These QTLs co-locate with the previously

153 described heading date QTLs *Eps-B1* and *Eps-D1* (Griffiths *et al.* 2009). In our data,
154 *Eps-B1* had a significant effect in both years, explaining 3.4% of genetic variance in
155 GS55 in 2013 and 2% in 2014 (Table 1). *Eps-D1* was also detected in both years but
156 only had an overall significant effect (–log10(p) = 2.32) in 2014, accounting for 4.1%
157 of genetic variance in GS55 in that year (Table 1). The *Eps-B1* and *Eps-D1 loci* were
158 chosen for further in-depth analysis because of their proximity to *ELF3* homoeologues.

159

160 *TaELF3-B1* is a candidate gene for the *Eps-B1* QTL

161 At the 1B QTL, the alleles derived from the MAGIC parents Soissons, Alchemy,
162 Robigus and Claire are associated with a relative reduction in the time to GS55,
163 indicated by the negative sign of the QTL, whilst alleles from Rialto, Hereward, Xi-19
164 and Brompton are associated with a delay to GS55, indicated by the positive sign of
165 the QTL (Table 2). The interval between the markers Ra_c109187_371 (296.34cM /
166 685.7Mb) and RAC875_c37075_283 (297.00cM / 687.7Mb) is 0.66cM, corresponding
167 to a physical length of ca. 2 Mb (Figure 2A).

168

169 The IWGSCv1.1 gene annotation suggests there are 26 high confidence gene models
170 within the interval of Ra_c109187_371 and RAC875_c37075_283. Based on current
171 gene annotation and orthology to cloned rice genes (Yao *et al.* 2018) there are no
172 novel candidates for the *Eps-B1* locus in addition to those described previously
173 (Faricelli *et al.* 2010, Alvarez *et al.* 2016, Zikhali *et al.* 2016). Compared to the *T.*
174 *monococcum* physical map of the *Eps-A^{m}1* region (Alvarez *et al.* 2016) *TmADK* (similar
175 to rice putative kinase *ADK1)* and *TmCK1-like* (*CASEIN KINASE I ISOFORM DELTA-*
176 *LIKE)* are not syntenic and the locus containing *TaELF3*, *TaGRIK1-like*
177 (*GEMINIVIRUS REP INTERACTING KINASE 1 LIKE*) and *TaPWWP1* (*PWWP*

178 *domain-containing protein*) is inverted (Figure 2A). Nineteen genes had
179 homoeologues on the syntenic 1D chromosome (Figure 2A).
180
181 Publicly available sequences for *TaELF3-B1* in Claire, Robigus (earlier heading
182 alleles) (Clavijo *et al.* 2017) and Rialto and Cadenza – the parents of Xi-19 - (later
183 heading alleles) (Zikhali *et al.* 2016) differed by one nonsynonymous SNP within exon
184 4 at position chr1B:685645813. No further nonsynonymous SNPs were identified from
185 the 820k SNP dataset from CerealsDB (Wilkinson *et al.* 2012), which contains all
186 MAGIC parents.
187
188 The SNP (Adenine at position 2020 of CDS to Guanine; A2020G) causes a predicted
189 deleterious amino acid substitution from the ancestral serine to a glycine residue at
190 position 674 of the predicted primary amino acid sequence (Ser674Gly; SIFT 0.01)
191 (Figure 2B). A KASP marker was designed for this SNP and used to genotype the
192 MAGIC population. The KASP marker mapped to the same genetic position as
193 Ra_c109187_371 and segregated with the predicted founder effects, confirming that
194 *TaELF3-B1* is part of the 1B GS55 QTL.
195
196 This predicted glycine at residue 674 of *TaELF3-B1*, associated with late heading, is
197 globally rare in wheat. In the 1000Exome data (He *et al.* 2019) 4.87% of lines have
198 the predicted glycine residue and in the wheat HapMap panel (Jordan *et al.* 2015),
199 only Rialto has the predicted glycine residue out of the 62 globally diverse lines
200 analysed (Supplemental Table S2). Similarly, of the 14 hexaploid varieties currently
201 available from the 10+ Wheat Genome project only three (Cadenza, Paragon,
202 ArinaLrFor) possess the non-ancestral glycine residue (Supplemental Table S2).
203 However, analysis of multiple datasets (see methods) found the non-ancestral

204 glycine674 is more common in wheat varieties with a UK pedigree (9/13 varieties)
205 (Supplemental Table S3). Alignment of *TaELF3* orthologues shows that the predicted
206 serine residue is also highly conserved across monocots (Supplemental Figure S1).
207
208 When looking for other potentially candidate sequence variation we found that within
209 the *ELF3-B1* promoter regions of Claire, Robigus, Paragon and Cadenza there are
210 two sites polymorphic for the number of repeated cytosines ($(C)_n$) located 1967 bp and
211 1151 bp upstream of the transcriptional start site (TSS) (Figure 2B). Variation in CT
212 repeat number within the 5'-UTR region of the wheat *cellulose synthase like* (*Csl*) gene
213 is associated with *Csl* expression and tiller number (Hyles *et al.* 2017). As Robigus
214 and Claire have an early heading phenotype at the *Eps-B1* locus and Cadenza a late
215 heading phenotype (Alvarez *et al.* 2016) it is unlikely that the promoter $(C)_n$
216 polymorphisms cause the changes in heading dates because there is only a difference
217 in two cytosines at the 1967 bp $(C)_n$ site between Cadenza and Robigus/Claire (Figure
218 2B). This conclusion is supported by our finding that there is no correlation between
219 the $(C)_n$ genotype and *TaELF3* expression (ANOVA $F = 0.484$, $p = 0.748$)
220 (Supplemental Figure S2). It was not possible to quantify the relative transcript
221 abundance of the *TaELF3-B1* homoeologue due to a lack of homoeologous SNPs in
222 the coding region of *TaELF3* as previously reported (Zikhali *et al.* 2016). Furthermore
223 *TaELF3-B1* in Julius, Lancer, Mace, Norin61 and Sy Mattis seems to be inverted
224 compared to ArinaLrFor, CDC Landmark, CDC Stanley, Chinese Spring and Jagger.
225 However, as none of these lines share the same haplotype with ArinaLrFor and
226 Paragon (which both carry the Ser674Gly SNP) at *ELF3-B1* it is unlikely that an
227 inversion is the cause behind the *Eps-B1* QTL. Thus, we conclude that the Ser674Gly
228 SNP in *ELF3-B1* is the best candidate to underlie *Eps-B1*.

229

230 Subtelomeric introgression and inversion might underlie 231 the *Eps-D1* heading date QTL

232 A subtelomeric deletion in Cadenza and Spark was previously described as the causal
233 polymorphism underlying the *Eps-D1* locus using Spark × Rialto, Avalon × Cadenza
234 mapping populations (Zikhali *et al.* 2016, Ochagavía *et al.* 2019). Our QTL analysis
235 for 2012 (Supplemental Table S1) and 2014 (Table 1) shows a minor QTL overlapping
236 this locus. In both years the Xi-19 founder genotype is associated with earlier heading
237 (2012: -1.26 days; p = 0.015; 2014; -0.79 days; p = 0.053). However correct genetic
238 map construction and resulting assignment of founder genotypes at this locus might
239 be more difficult given the high-density marker region previously identified at the end
240 of 1D. These high-density marker regions were hypothesised to be associated with
241 introgressions (Gardner et al., 2016). Based on the previously reported deletion in
242 Cadenza and Spark (Zikhali, Wingen, and Griffiths 2016) and the pedigree of Xi-19
243 (Cadenza/Rialto//Cadenza) we hypothesised that the Cadenza allele inherited from
244 Tonic was a likely candidate for the observed QTL effects. By analysing data from
245 recently published wheat assemblies (Walkowiak *et al.* 2020) we suggest the
246 polymorphism is due to a subtelomeric inversion derived from introgressed material
247 rather than a deletion. A BLAST search of the Chinese Spring *TaELF3-D1* genomic
248 sequence against the 10+ Wheat Genome Project varieties identified high confidence
249 matches in all varieties including Cadenza. Interestingly, the sequence retrieved from
250 the variety Jagger was identical to Cadenza. However, the sequence identity of the
251 Jagger and Cadenza coding sequence for TraesJAG1D01G492900.1 and
252 TraesCAD_scaffold_026352_01G000400.1 compared to the Chinese Spring gene is
253 much lower (96.72%) than for the remaining 1D coding sequences (>99.9%). The

254 Jagger and Cadenza 1D coding sequences have a greater similarity to the Chinese
255 Spring *TaELF3-A1* (97.50%) and Chinese Spring *TaELF3-B1* (97.88%)
256 homoeologues than to Chinese Spring *TaELF3-D1*.
257
258 Visualisation of the 1D chromosome for the 10+ Wheat Genome Project varieties using
259 the Crop Haplotypes viewer (Brinton *et al.* 2020) showed a shared haplotype block at
260 the distal end of chromosome 1D between Cadenza (Haplotype viewer coordinates:
261 482.8 Mbp – 495.4 Mbp) and Jagger (480.0 Mbp to 493.5 Mbp) where *TaELF3-D1* is
262 found.
263
264 The Cadenza v1.1 reference sequence has yet to be assembled into chromosomes,
265 but since the Crop Haplotypes viewer (Brinton *et al.* 2020) data indicated identical by
266 state (IBS) haplotypes between Jagger and Cadenza, we compared the distal end
267 structure of the Jagger 1D chromosome with Chinese Spring. The end of the Jagger
268 chromosome contains an inversion of approximately 2.6 Mbp relative to Chinese
269 Spring which includes *TaELF3-D1* (Figure 3A). Alignment of the Jagger/Cadenza
270 *TaELF3-D1* genomic sequence with Chinese Spring *TaELF3-D1* showed some
271 sequence differences including a deletion within intron 2 (Figure 3B, Supplemental
272 Table S4). We developed a subgenome specific PCR assay detailed in Figure 3B that
273 amplifies the region of *TaELF3-D1* containing intron 2 and used this as a simple
274 marker for the 1D introgression. We confirmed that of the eight MAGIC parents, only
275 Xi-19 carried the Cadenza/Jagger *TaELF3-D1* allele (Figure 3C and D). As
276 hypothesised Spark and Tonic also carry the Cadenza *TaELF3-D1* allele (Figure 3C,
277 D and Supplemental Figure S3) as well as the varieties Maris Fundin and Cordiale
278 which show introgression signatures on the distal end of chromosome 1D (Scott *et al.*

279 2021). A simplified pedigree diagram shows how some of the cultivars are related
280 (Supplemental Figure S4). The intron 2 deletion is also present in *Aegilops speltoides*
281 and *Triticum timopheevii* (Supplemental Figure S5).
282
283 Given the low sequence conservation of the *TaELF3-D1* gene in Cadenza and Jagger
284 and the presence of the intronic deletion in *Aegilops speltoides* and *Triticum*
285 *timopheevii*, we investigated the wider phylogeny of the 1D Jagger/Cadenza region
286 using the 820k SNP dataset from CerealsDB. This showed that Cadenza, Xi-19 and
287 Spark as well as several other Tonic descendants (KWS-Podium, Cordiale, Gallant,
288 Duxford) and five other cultivars (Moisson, Bacanora, Tuerkis, Badger, Pavon)
289 clustered separately from the remaining *T. aestivum* cultivars (Supplemental Figure
290 S6). These lines also cluster with six Watkins lines from India (Watkins34), Yugoslavia
291 (Watkins352), China (Watkins141), UK (Watkins103), Cyprus (Watkins292) and
292 Turkey (Watkins299). *T. timopheevii* clusters closely with the above lines. Gene
293 alignment of *ELF3-D1* orthologues and alignment of 300 kb surrounding *ELF3-D1* also
294 supports an origin outside the D genome for the Jagger/Cadenza *ELF3-D1* gene
295 (Supplemental Figure S7, Supplemental Table S5).
296

297 Allelic variation in *TaELF3* had no detectable effect on 298 circadian rhythms in the MAGIC parent varieties

299 We investigated if the variations at *TaELF3-B1* and *TaELF3-D1* in the MAGIC parents,
300 or other *loci,* might be associated with alterations of circadian rhythms in a manner
301 that might explain the effects on heading date. We quantified circadian rhythms in the
302 MAGIC parent varieties by measuring the period and amplitude of rhythms of delayed
303 chlorophyll fluorescence (DF) in otherwise constant light (Gould *et al.* 2009). There

304 were robust circadian rhythms of DF in all the MAGIC parent lines (RAE < 0.5) (Figure
305 4A). Hereward had the shortest circadian period (25.0 h) (Figure 4C) and Xi-19 the
306 longest period (26.2 h) but the difference between these periods and the mean of all
307 parents was not significant (p = 0.132) (Figure 4C). To determine whether the lack of
308 an altered circadian phenotype in the MAGIC parent lines was the result of masking
309 by compensatory alleles at other *loci,* we selected some of the earliest and latest
310 heading MAGIC RILs from 2014 and used chlorophyll *a* fluorescence (PF) to measure
311 circadian rhythms in continuous light (Supplemental Figure S8). There was no
312 significant relationship between heading (early or late) and circadian period (p =
313 0.4216) (Supplemental Figure S8B) or between heading and circadian rhythm
314 amplitude (p = 0.7385) (Supplemental Figure S8C). We detected robust rhythms of PF
315 in all lines (RAE < 0.5) (Supplemental Figure S8D) indicating that in these lines there
316 was no effect on circadian rhythm robustness. We then investigated whether there
317 was any significant relationship between circadian rhythm parameters and the *ELF3-*
318 *B1, ELF3-D1* or *Ppd-1* alleles associated with altered heading date. There was no
319 significant difference between circadian period and *ELF3-B1* alleles (p = 0.542), *ELF3-*
320 *D1* alleles (p = 0.521) or *Ppd-1* alleles (0.507). Similarly, there was no significant
321 difference between circadian amplitude and *ELF3-B1* alleles (p = 0.942), *ELF3-D1*
322 alleles (p = 0.1302) and *Ppd-1* alleles (0.966). Thus, the allelic diversity in
323 homoeologues of *TaELF3* that was associated with alterations in heading date did not
324 cause detectable changes in circadian rhythms.
325

326 *TtELF3* has separable effects on heading date and the wheat
327 circadian clock

328 Because allelic variation of *TaELF3* was associated with heading date but not
329 circadian rhythms in the MAGIC parents and RILs, we examined directly whether *ELF3*
330 affects heading and is a circadian clock component in wheat by examining tetraploid
331 TILLING mutant lines carrying point mutations encoding stop codons in both *TtELF3-*
332 *A1, TtELF3-B1* or both (Alvarez *et al.* 2016) (Supplemental Figure S9). The *Ttelf3*-null
333 line headed first (48.7 days) with *TtELF3*-WT heading significantly ($p < 0.0001$) later
334 (56.4 days) as previously reported (Alvarez *et al.* 2016). There was no significant
335 difference ($p = 0.98$) in heading date between *Ttelf3*-Anull (51.0 days) and *Ttelf3*-Bnull
336 (52.4 days) suggesting that the *TtELF3-A* and *TtELF3-B* homoeologues contribute
337 equally to heading date. However, they were both significantly later heading than
338 *Ttelf3*-null ($p < 0.0001$) and significantly earlier than *TtELF3*-WT ($p < 0.0001$).
339
340 We found that functional *ELF3* is required for robust circadian rhythms in continuous
341 light and that single wild type *ELF3* homoeologues can maintain circadian function in
342 the absence of other functional homoeologues. There were robust circadian rhythms
343 of $F_{m'}$ in *TtELF3*-WT (RAE 0.16 ± 0.05), *Ttelf3*-Anull (RAE 0.14 ± 0.04) and *Ttelf3-*
344 Bnull (RAE 0.15 ± 0.07) but no robust circadian rhythms in *Ttelf3*-null (RAE 0.53 ±
345 0.19) (Figure 5B-C). The arrhythmic phenotype of *Ttelf3*-null was confirmed using DF
346 and leaf temperature measurements (Supplemental Figure S10A-F) and was not the
347 result of reduced maximum quantum yield of photosystem 2 (F_v/F_m) as this was higher
348 for *Ttelf3*-null for the duration of measurement (Supplemental Figure S10G-I). There
349 was no significant difference in circadian period of $F_{m'}$ ($p > 0.05$) between *TtELF3*-WT
350 (24.4 h ± 1.2), *Ttelf3*-Anull (24.3 h ± 0.7) and *Ttelf3*-Bnull (24.9 h ± 1.0). Similarly, there
351 was no significant difference ($p > 0.05$) in the amplitude of $F_{m'}$ oscillations between
352 *TtELF3*-WT (241 ± 53), *Ttelf3*-Anull (218 ± 50) and *Ttelf3*-Bnull (236 ± 57).

353

354 Our results demonstrate that allelic variation at individual *ELF3* homoeologues is
355 sufficient to alter heading date without affecting circadian rhythms, indicating that *ELF3*
356 has separable effects on heading date and the circadian clock in wheat.

357

358 Loss of functional *TtELF3* perturbs circadian oscillator gene 359 expression in light/dark cycles and constant light

360 To further investigate the function of *ELF3* in the wheat circadian system we measured
361 the relative transcript abundance of orthologues of the Arabidopsis circadian oscillator
362 components *LHY, TOC1, Ppd-1* (*PRR37*)*, PRR73, GI, ELF3* and *LUX* in light dark
363 (LD) and continuous light (LL) cycles. In LD cycles all transcripts had rhythmic
364 expression (Figure 6A-G). Consistent with previous findings in Arabidopsis, *TtLHY* had
365 peak expression at dawn (Figure 6A), the *PRR* orthologues peaked during the
366 photoperiod (Figure 6B-C) with *TtTOC1* (Figure 6D), *TtGI* (Figure 6E) and *TtLUX*
367 (Figure 6F) peaking around dusk. However, the peak in *TtELF3* abundance was at the
368 end of the night just prior to dawn (Figure 6G), approximately antiphase to the
369 expression of *TtLUX* (Figure 6F). This differs markedly from Arabidopsis in which *ELF3*
370 and *LUX* are co-expressed near dusk (Nusinow *et al.* 2011, Huang *et al.* 2016, Ezer
371 *et al.* 2017). For all transcripts, except *Ppd-1* (Figure 6B), we detected oscillations in
372 relative transcript abundance in constant light, with the phasing in LL consistent with
373 that in LD. These oscillations of circadian transcript abundance were abolished, or of
374 very low amplitude, in *Ttelf3*-null (Figure 6A-G). Interestingly, the expression of *Ppd-1*
375 was consistently higher in *Ttelf3*-null in both LD and the first LL cycle (Figure 6B) and
376 the minimum level of the *Ppd-1* homologue *TtPRR73* was also higher in *Ttelf3*-null in

377 LD (Figure 6C) which suggests that ELF3 might act as negative regulator of *Ppd-1*
378 and *TtPRR73.*
379
380 There was a phase advance in peak transcript abundance of approximately 3 h in LD
381 in *Ttelf3*-null compared to *TtELF3-WT* (Figure 6A-G) except for *TtELF3* transcript
382 abundance where the peak phase was at dawn in both *TtELF3*-WT and *Ttelf3*-null
383 (Figure 6G). The amplitude of transcript abundance under diel conditions was also
384 less in the *Ttelf3*-null line compared to *ELF3*-WT (Figure 6). Together, these data
385 demonstrate that functional *TtELF3* is required for the maintenance of robust
386 oscillations of circadian oscillator gene expression in LL and for normal circadian
387 timing in LD.
388
389

390 *LUX* loss of function disrupts the wheat circadian clock

391 The antiphase expression of wheat *ELF3* and *LUX* raises the possibility that the EC
392 might not be formed, or functions differently to that in Arabidopsis. Previous studies in
393 diploid wheat have identified *TmLUX* as a circadian oscillator gene (Gawronski *et al.*
394 2014), so we investigated whether *LUX* also contributes to circadian rhythms in
395 hexaploid wheat, and whether functionality of one homoeologue is sufficient to
396 maintain robust oscillations. We obtained three hexaploid Japanese cultivars,
397 Chogokuwase, Minaminokomugi and Geurumil that have variation at *TaLUX*
398 associated with flowering time (Mizuno *et al.* 2012). Chogokuwase is an extra early
399 flowering variety and is the offspring of Geurumil and Minaminokomugi. Chogokuwase
400 carries predicted non-functional mutations in all three sub-genome copies of *TaLUX*
401 (Supplemental Figure S11). Chogokuwase also carries a *TaVRN-D1* spring allele and

402 a photoperiod insensitive *Ppd-D1a* allele. Geurumil has the same predicted non-
403 functional alleles of *TaLUX* and *Ppd-D1a* but has a winter growth habit due to lacking
404 the *VRN-D1* spring allele. Minaminokomugi carries the non-functional *Talux-a1* allele
405 but wild-type alleles of *TaLUX-B1* and *TaLUX-D1* in addition to carrying the *TaVRN-*
406 *D1* and *Ppd-D1a* alleles (Mizuno *et al.* 2016).
407
408 Minaminokomugi maintained robust oscillations of chlorophyll fluorescence (RAE 0.16
409 ± 0.01) and leaf temperature (RAE 0.26 ± 0.02) (Figure 7A-C). In contrast
410 Chogokuwase, which lacks functional copies of *TaLUX,* was arrhythmic for PF (RAE
411 0.56 ± 0.06) and Geurumil, which is also lacking functional *TaLUX*, had reduced
412 robustness of PF oscillations (RAE 0.33 ± 0.05) compared to Minaminokomugi (Figure
413 7A-C). Similarly, there was a decreased robustness of oscillations in leaf surface
414 temperature for Chogokuwase and Geurumil (RAE 0.48 ± 0.09 and RAE 0.46 ± 0.11)
415 which appeared to dampen to arrhythmia after the first two true LL cycles (Figure 7D-
416 F). We conclude that functional *TaLUX* is required for robust circadian rhythms in
417 hexaploid wheat.
418

419 # Discussion

420 ## Wheat *ELF3* contributes to heading date and circadian
421 ## rhythms independently

422 The eight MAGIC parent varieties provided the opportunity to measure the likely
423 contribution of the *ELF3* homoeologues to heading date and circadian rhythms. Of the
424 MAGIC parents Brompton, Hereward, Rialto and Xi-19 have a G|G substitution variant
425 of *TaELF3-B1* and in addition Xi-19 has an inverted copy of *TaELF3-D1,* likely arising

426 from a past introgression event. These variations in *TaELF3* alleles had no discernible
427 impact on circadian rhythms (Figure 4) but were associated with measurable effects
428 on heading date in the field (Supplemental Figure S12).
429
430 Consistent with previous studies, *ELF3* is a candidate for *Eps-D1 loci* (Zikhali *et al.*
431 2016). We have extended the findings concerning the *Eps-D1* locus by demonstrating
432 that rather than being within a deletion, a copy of *ELF3-D1* is present in Cadenza (as
433 well as Xi-19, Spark, Cordiale, Tonic and Maris Fundin) but does carry candidate
434 sequence variations. *ELF3-D1* lies within an introgression region that contains an
435 inversion relative to the Chinese Spring D genome (Figure 3) and current data cannot
436 rule out other candidate genes within the introgression and/or inversion region. Based
437 on analysis of the 820k SNP data we find that several descendants of the cultivar
438 Tonic carry the putative introgression, as do several other unrelated cultivars and six
439 Watkins lines from India, China, UK, Cyprus, Turkey, and Yugoslavia. The
440 introgression is also likely present within Chinese elite germplasm (Wang *et al.* 2016).
441 As a result, we hypothesise that this region predates modern breeding efforts. The
442 same genomic region has been identified as being under selection in a collection of
443 bread wheat accessions dating from 1790 to 1930, though in that study it was
444 presumed to be a deletion rather than introgression (Przewieslik-Allen *et al.* 2021).
445 While the origin of the introgression is uncertain, the presence of the Jagger/Cadenza
446 *TaELF3-D1* intronic deletion in *Ae. speltoides* and *T. timopheevii* (Supplemental
447 Figure S5) and the clustering outside of *Aegilops tauschii* lines (Supplemental Figure
448 S6 and Supplemental Figure S7) supports an origin outside of the D genome, more
449 closely related to the G or S genome. The increase in quantity and quality of genomic

450 resources for diverse accessions and wheat relative species will help in determining
451 the origin of this introgression.
452
453 Our data also identify *TaELF3-B1* as a candidate gene underlying the *Eps-B1* locus.
454 We found that a predicted glycine674 (G|G) in *TaELF3-B1,* which segregates with
455 *Eps-B1,* caused a delay in heading and flowering compared to the ancestral serine674
456 variant (A|A) (Supplemental Figure S12), in agreement with previous observations in
457 Avalon (Zikhali *et al.* 2016). It was previously concluded that G|G is the ancestral
458 variant (Zikhali *et al.* 2016) but our evidence suggests that it is more likely that A|A is
459 ancestral because the G|G allele is globally rare, present in 4.87% of lines included in
460 the 1000 Exome dataset, in one of the 62 wheat HapMap panel lines (Supplemental
461 Table S2) and in three of the 14 10+ Wheat Genome project lines (Supplemental Table
462 S2) and the ancestral serine residue is highly conserved, present in all sequenced
463 grasses. However, within UK wheat germplasm (as defined by locality on wheat GRIS)
464 the G|G allele is more common and is found in nine of the 13 UK lines we have
465 investigated (Supplemental Table S3). The later flowering G|G allele may be more
466 favoured in northern regions (Langer *et al.* 2014).
467
468 We found that the allelic variation at *TaELF3* had no detectable effect on circadian
469 rhythms in the MAGIC parents or early and late heading RILs. Epistasis between *ELF3*
470 and *Ppd-D1* has previously been reported for flowering time (Faure *et al.* 2012, Alvarez
471 *et al.* 2016). However, we find that variation at *Ppd-A1* has no effects on circadian
472 rhythms or modification of circadian phenotypes in *Ttelf3*-nulls (Supplemental Figure
473 S13). We also find no evidence of epistasis between *eps-B1* and *eps-D1* in the

474 regulation of circadian rhythms because Xi-19 has both *eps-B1* and *eps-D1* but was
475 not distinguishable from the rest of the population in terms of circadian behaviour.
476
477 Using loss of function lines, we demonstrate that *ELF3* regulates heading and is
478 required for circadian rhythms in wheat. Whilst complete loss of functional *TtELF3*
479 caused arrhythmia of PF (Figure 5B-E & Supplemental Figure S10G-I), leaf
480 temperature (Supplemental Figure S10D-F) and gene expression in LL (Figure 6), loss
481 of function of either the A or B homoeologue was without effect on circadian rhythms
482 if the other homoeologue was functional (Figure 5B-E). This contrasts with the effect
483 on heading, where loss of either the A or B homoeologue function resulted in an
484 advance in heading date relative to wildtype and the magnitude of this advance was
485 intermediate relative to the double null mutant (Figure 5A). These results, coupled with
486 the increased expression in *Ttelf3*-null of the floral promoter *Ppd-1* (Figure 6B) and
487 *FT1* (Supplemental Figure S14), suggest that wheat *ELF3* functions as a core
488 circadian oscillator component whilst also having a direct effect on flowering
489 independent of its role in the circadian oscillator (Figure 8).
490
491 Loss of functional *TtELF3* advanced circadian phase in LD. This demonstrates that
492 one role of *ELF3* is to contribute to the correct alignment of internal phase to external
493 phase, which is a primary function of circadian oscillators. The earlier phasing of gene
494 expression in LD cycles is similar to barley containing the *eam8.*w allele where the
495 peak phase of *HvCCA1, HvTOC1* and *HvGI* expression was also earlier (Faure *et al.*
496 2012). Similarly, the same study reported loss of rhythmic oscillations in gene
497 expression upon transition to LL in barley. We found that functional *TtELF3* is required
498 for high amplitude *TtLHY* rhythms, and that *TtELF3* loss of function mutants have

499 increased trough transcript abundance of *TtGI* (Figure 6E). The similarity of these
500 observations to those in barley and rice lines carrying *ELF3* mutations (Zhao *et al.*
501 2012, Boden *et al.* 2014) suggests that *ELF3* genes might have similar functions
502 across grasses.
503
504 Wheat PHYTOCHROME B (PHYB) and PHYC are required for accelerated heading
505 in long days (Chen *et al.* 2014, Pearce *et al.* 2016, Kippes *et al.* 2020, Bouché *et al.*
506 2022) and PHYB and PHYC are required for the induction of *Ppd*-1 expression during
507 night-breaks in wheat (Pearce *et al.* 2017). In Arabidopsis PHYB co-locates at sites
508 bound by the EC (Ezer *et al.* 2017) and in Brachypodium ELF3 appears to affect PHYC
509 activation of *Ppd-1* physical interaction (Gao *et al.* 2019). Together these results
510 support the hypothesis that wheat ELF3 may act as an integrator of light signalling
511 downstream of the phytochromes and upstream of Ppd-1 (Kippes *et al.* 2020) placing
512 it within one of the wheat photoperiod pathways (Shaw *et al.* 2020) (Figure 8).
513

514 An altered role for the evening complex (EC) in wheat

515 Binding of the Arabidopsis EC to target promoters requires LUX, as both ELF3 and
516 ELF4 lack DNA binding domains, and it is thought this might explain the similar timing
517 of the transcript accumulation (Nusinow *et al.* 2011). However, in wheat the maximal
518 abundance of *ELF3* and *LUX* transcripts is separated by 12 hours (Figure 6F and G).
519 This difference in the peak time of *ELF3* and *LUX* transcript abundance also occurs in
520 *T. monococcum* (Alvarez *et al.* 2016), rice (Zhao *et al.* 2012) and between *ELF3-like1*
521 and *LUX* in maize, sorghum and foxtail millet (Lai *et al.* 2020). This suggests that
522 temporal separation of *ELF3* and *LUX* expression might be a general feature of cereal
523 circadian oscillators. Wheat also lacks a clear orthologue of *AtELF4* and instead

524 contains *ELF4-like* genes (Calixto *et al.* 2015). *ELF4-like* genes might have a
525 conserved role because expression of a barley *ELF4-like* gene restored circadian
526 rhythms to an Arabidopsis *elf4-2* mutant (Kolmos *et al.* 2009). There is further
527 evidence for conservation of EC function in monocots because Brachypodium ELF3
528 binds Arabidopsis ELF4 and LUX, and can complement Arabidopsis *elf3-2* mutants
529 (Huang *et al.* 2017). The temporal separation of wheat *ELF3* and *LUX* transcript
530 abundance does not preclude the formation of an EC complex, but could suggest one
531 is not formed, or occurs at a different time in the diel cycle to Arabidopsis. Whether
532 through an EC or not, our data demonstrate that functional *ELF3* and *LUX* are required
533 for robust circadian rhythms in wheat (Figures 6- 8).
534
535 Whilst it is notoriously difficult to attribute plant promoter *cis*-elements to specific
536 patterns of expression (Harmer and Kay 2005), the difference in timing of *TaELF3* and
537 *TaLUX* expression compared to their Arabidopsis orthologues might arise because of
538 promoter sequence differences. Within 5000 bp upstream of the three *TaELF3*
539 homoeologues transcription start sites the most common motifs are linked to morning
540 phased expression (37 morning, 20 evening and 7 midnight) (Supplemental Table S6).
541 The general composition of the *TaELF3* promoters is similar to *TaLHY* (22 morning, 9
542 evening and 3 midnight) (Supplemental Table S7) but different to the evening
543 expressed *TaLUX* promoters where the most abundant motifs are associated with
544 evening phased expression (32) compared to morning (23) and midnight (12)
545 (Supplemental Table S8). In particular*, TaELF3* promoters contain Morning Element
546 1 (ME1) and Morning Element 2 (ME2) motifs, associated with morning phased
547 expression (Michael *et al.* 2008), which are also found in the promoter region of the
548 dawn expressed *TaLHY* homoeologues (Supplemental Table S7) but are absent in

549 the *AtELF3* promoter (Supplemental Table S6). The *TaELF3* promoters also contain
550 further morning-related motifs such as the multiple Hormone up at dawn 1 (HUD1) and
551 Hormone up at dawn 2 (HUD2) elements (Michael *et al.* 2008) which are less frequent
552 in the *AtELF3* promoter (Supplemental Table S6).
553

554 Wheat *ELF3* might be a promising breeding target

555 *ELF3* might be a suitable target for breeding new lines with heading date better
556 adapted to the local environment in the practice of chronoculture (Steed *et al.* 2021).
557 In other species such as pea, lentil and barley, allelic variation in *ELF3* has permitted
558 the cultivation of these crops at different latitudes (Weller *et al.* 2012, Zakhrabekova
559 *et al.* 2012, Lundqvist 2014). Whilst complete loss of functional *ELF3* in wheat
560 significantly advances flowering time, severely disrupts circadian rhythms and
561 decreases the spikelet number (Alvarez *et al.* 2016), we have demonstrated that
562 altering the function of particular homoeologues of *ELF3* can affect heading without a
563 measurable disruption to the circadian oscillator (Figure 5) and the potential
564 associated yield penalties (Dodd *et al.* 2005), providing some functional copies of
565 *ELF3* are present. It might be possible by combining different alleles of *ELF3* with
566 alleles of other circadian clock genes, to precisely tune flowering time suited to the
567 growing environment. This could be tested by measuring flowering time in selected
568 Cadenza TILLING lines (Krasileva *et al.* 2017) containing mutations in other circadian
569 clock genes as Cadenza contains both the *TaELF3-B1* Ser674Gly SNP and the 1D
570 introgression. In addition to the *ELF3* alleles described in this work, we have also
571 identified further *ELF3* alleles including the absence of *ELF3-A1* in Julius
572 (Supplemental Table S9) highlighting a range of *ELF3* alleles within modern wheat
573 cultivars which could be incorporated into breeding programmes. The variation at

574 *ELF3* might have occurred because of the positioning of *ELF3* within the subtelomeric
575 region (Aguilar and Prieto 2020) which has enhanced levels of recombination which
576 can lead to increased number of sequence and structural variants. This has been
577 observed for other regions, recent studies have reported that a deletion at the distal
578 end of chromosome 4AL is associated with altered heat tolerance (Zhai *et al.* 2021)
579 and a deletion at the distal end of 5AL encompasses the *Rht12* locus which is
580 associated with dwarfing (Sun *et al.* 2019). Secondly, variation at *ELF3* may have been
581 selected by past breeding efforts, leading to a change in allele frequencies, due to
582 advantageous adaptation of flowering time to local climates similar to that seen for
583 selection of *Ppd-1* alleles based on latitudinal cline (Cockram *et al.* 2007) and altitude
584 (Guo *et al.* 2020). A more systematic understanding of circadian clock gene alleles
585 and their combinations will allow for a more targeted approach in optimising flowering
586 time without impacting the functioning of the circadian clock.
587

588 # Materials and methods

589 ## Plant material

590 The eight MAGIC parents; Alchemy, Brompton, Claire, Hereward, Rialto, Robigus,
591 Soissons and Xi-19 were obtained from NIAB (National Institute of Agricultural Botany,
592 UK). The *Ttelf3*-null and *TtELF3*-WT lines were donated by Jorge Dubcovksy (Alvarez
593 *et al.* 2016) where the *Ttelf3*-null line is the progeny of bulked *elf3-null/Ppd-A1b* and
594 the *TtELF3*-WT line is progeny of bulked *ELF3WT/Ppd-A1b* (Table 4). By outcrossing
595 we selected lines that contained just the *Ttelf3-A1* mutation (herein *Ttelf3*-Anull) or just
596 the *Ttelf3-B1* mutation (*Ttelf3*-Bnull). The Chogokuwase, Minaminokomugi and
597 Geurumil lines were donated by Hidetaka Nishida (Mizuno *et al.* 2012).
598

599 ## Plant growth conditions

600 Seeds were surface sterilised by washing once in 70% (v/v) ethanol for one minute
601 (Fischer Scientific, UK), once in autoclaved water for one minute, followed by 15
602 minutes in 10% (v/v) sodium hypochloride solution (Fischer Scientific, UK) and then
603 washed a further three times in autoclaved deionised water. Seeds were sown directly
604 onto 96 well modular trays (P G Horticulture Ltd, UK), containing a 1:1 mix of Levington
605 M2 potting compost (Levington, UK) and vermiculite (fine, Willian Sinclair Horticulture,
606 UK) and treated with the insecticide Intercept 70W (0.02 g L-1 soil, Bayer, Germany).
607 Plants were grown in growth chambers (Conviron, Canada) under long days and
608 constant temperature (16 h L: 8 h D; 200 µmol m^{-2} s^{-1}; 20 °C or 16 h L: 8 h D; 400
609 µmol m^{-2} s^{-1}; 22 °C) or in growth cabinets (see specific methods).
610

611 ## Field trials

612 In 2012/2013 a fully replicated yield trial of 784 F_5 MAGIC lines at the NIAB
613 experimental farm in Cambridge, UK was scored by NIAB for the timing of Growth
614 Stages on the Zadok's scale (Zadoks *et al.* 1974, Mackay *et al.* 2014). Each plot was
615 assessed every two days for its growth stage based on representative plants at the
616 centre of each plot. Once a plot reached GS55 (half of ear emerged above flag leaf
617 ligule) the date was logged. The phenotype was assessed with growth stage
618 measurements scored as days after sowing. In the 2013/2014 field season the same
619 growth stage phenotypes were collected from a fully replicated yield trial of 784 F_6
620 MAGIC lines.
621

622 ## Analysis of field phenotypes

623 Asreml-R 3.0 (Gilmour *et al.* 1997) was used to minimise or remove spatial effects in
624 phenotype data due to field variation.
625
626 Marker genotypes and their respective chromosomal groupings from (Gardner *et al.*
627 2016) were used. The genetic map was reordered visually using the R package
628 mpMapInteractive (Shah 2013) to improve ordering and consider physical ordering
629 information from IWGSCRefSeqv1. Recombination fractions were recalculated in
630 mpMap (Huang and George 2011) for each chromosome using mpestrf().
631 Recalculating recombination fractions on a per chromosome basis with the existing
632 marker groupings significantly reduced computation resources required and enables
633 the use of finer recombination bins (r <- c(0:5/600, 2:20/200, 11:50/100) compared to
634 the default values. Genetic map lengths were recalculated using the Kosambi mapping
635 function in computemap().
636
637 To reduce computational effort a skimmed genetic map with only unique mapping
638 locations was used to calculate the probability that each location on a genome was
639 inherited from each parent and conduct QTL mapping in MPWGAIM only (Verbyla *et*
640 *al.* 2014). A marker for each unique coordinate was chosen which had the lowest
641 missing calls and preferably a clear BLAST hit to the IWGSCRefSeqv1 reference
642 sequence, which was used to assign physical mapping coordinates. Out of 18089
643 mapped markers 4458 were chosen for founder probability calculations.
644
645 To test and validate our pipeline and analysis tools we used them to interrogate a data
646 set describing flowering time in a 2011/2012 nursery of the NIAB eight Parent MAGIC
647 population that had previously been analysed using Bayesian Networks (Scutari *et al.*
648 2014). Reanalysis of this data using MPWGAIM (Verbyla *et al.* 2014) detected 13

649 significant QTLs for flowering time with significant founder effects (Supplemental Table
650 S1).
651
652 This analysis identified a major QTL (18.3% genetic variation explained, LOGP 18.33)
653 between the markers Kukri_c27309_590 (48.57 cM) and BS00064538_51 (56.64 cM),
654 defining a maximum mapping interval of 31.81 Mb – 34.23 Mb between the two
655 mapping bins as several markers map to the 56.64 cM bin. The mean founder effects
656 of the QTL predict a significant acceleration of flowering time for Soissons, which is
657 the only parent carrying the photoperiod insensitive *Ppd-D1a* allele (Bentley *et al.*
658 2013) and furthermore *Ppd-D1* maps within the QTL (33.95 Mb). This analysis of the
659 effect of *Ppd-D1a* on flowering time validated MPWGAIM and our QTL mapping
660 pipeline in MAGIC.
661

662 Synteny analysis between Chinese Spring and Jagger 1D

663 A conserved haplotype block between Cadenza and Jagger at the distal end of
664 chromosome 1D was identified using the Crop Haplotypes web browser (Crop
665 Haplotypes (crop-haplotypes.com) (Brinton *et al.* 2020). Physical locations of genes
666 on the Chinese Spring 1D chromosome (IWGSCRefSeqv1.1) and Jagger 1D
667 chromosome (PGSBv2.0) were mapped using the mapviewer v2.6.1
668 (https://10wheatgenomes.plantinformatics.io/mapview) and then confirmed manually
669 using EnsemblPlants.
670

671 SNP mining and analysis

672 820k and 35k SNP array data was obtained from the CerealsDB website (Wilkinson
673 *et al.* 2012) and the 1000Exome data from the 1000 Exomes project website

674 (http://wheatgenomics.plantpath.ksu.edu/1000EC/). Mapping of 35k and 820k SNPs
675 to the IWGSCv1.1 Ref sequence were obtained from EnsemblPlantsv51. SNPs for the
676 Cadenza/Jagger haplotype (chr1D: 482.3Mb – end of chromosome 1D) were
677 extracted and heterozygous calls set as missing. Distance matrices and phylogenetic
678 trees were constructed using the R package "ape" (Paradis and Schliep 2019) 100
679 bootstrap permutations were run also using the R package "ape".
680
681 To investigate the prevalence of the Ser674Gly SNP in a broad range of germplasm
682 we analysed variation data from multiple sources including the 820k SNP genotyping
683 array (Winfield *et al.* 2016), the wheat HapMap panel (Jordan *et al.* 2015), the 1000
684 wheat Exome project (He *et al.* 2019) and the 10+ Wheat Genome project (Walkowiak
685 *et al.* 2020). We found that the Ser674Gly SNP was also present in the HapMap panel
686 as chr1B_685645813 and within the 1000 Exome data as scaffold48561_337271.
687

688 ## Phylogenetic tree construction

689 *ELF3-D1* orthologous groups were retrieved from public repositories. Coding
690 sequences were aligned using the MCoffee aligner on default settings
691 (https://pubmed.ncbi.nlm.nih.gov/16556910/). Maximum Likelihood (ML) Phylogenetic
692 trees were build using CLC Genomics Workbench 21.0.3. The best substitution model
693 was determined using the Model testing function before running Molecular
694 Phylogenetic analysis by Maximum Likelihood method with 100 permutations for
695 Bootstrap values. The *ELF3* gene from *Brachypodium distachyon* was used as an
696 outgroup.
697

698 ## Quantitative Real-Time PCR

699 The *TtELF3*-WT and *Ttelf3*-null lines were sown and grown in two antiphased LED
700 growth chambers (Conviron) under long day conditions (16h L: 8h D; 250 µmol m^{-2} s^{-}
701 ^{1}, 20°C day: 16°C night). Sampling commenced 16 days post-sowing, the first true
702 leaf was sampled every 3 hours for 96 hours. After the first 24 hours of sampling the
703 cabinet was switched to constant light and temperature (250 µmol m^{-2} s^{-1}, 20°C). Total
704 RNA was extracted from leaf samples using the KingFisher Flex purification system
705 (Thermofisher scientific) in conjunction with the Maxwell® HT simplyRNA Kit
706 (Promega). RNA concentration was determined using the Nanodrop ND-1000. DNA
707 contamination was removed using the Arcticzyme HL-DNAse kit. RNA integrity was
708 checked using the Fragment AnalyzerTM (AATI, USA) before cDNA was synthesised
709 from extracted RNA using the High-Capacity cDNA reverse transcription kit (Applied
710 Biosystems). Three technical replicates of gene specific products were amplified in 10
711 µl reactions using Power SYBR Green Master mix on a CFX384 Touch Real-Time
712 PCR detection system. Gene expression levels were determined relative to the
713 expression of two housekeeping genes, *RP15* and *RPT5A,* that were selected using
714 the GeNorm alogorithm (Vandesompele *et al.* 2002) (Table 5).
715
716 For quantification of *TaELF3* transcript abundance Cadenza, Chinese Spring, Claire,
717 Paragon and Robigus seed was sown and grown in a Conviron growth room (16h L:
718 8h D; 400 µmol m^{-2} s^{-1}, continuous 22°C. After 14-days leaf samples were taken and
719 RNA extracted using the RNAeasy plant mini kit (Qiagen, UK) with an on column
720 DNAse digest (Qiagen, UK). RNA concentration was determined on the Nanodrop ND-
721 1000 and cDNA synthesised from 500 ng RNA using the RevertAid First Strand cDNA
722 synthesis kit (Thermo Scientific, UK). Technical duplicates of gene-specific products

723 were synthesised in 10 µl reactions using the Rotor-Gene SYBR Green PCR kit
724 (Qiagen, UK) on a Rotor-Gene 6000 Real-Time PCR machine (Qiagen, UK).
725

726 PCR of *ELF3-D1*

727 DNA extracted using the DNeasy plant mini extraction kit (Qiagen, UK). The presence
728 of *ELF3-D1* was confirmed by PCR using the *TaELF3-D1* primers listed in Table 5.
729 PCR was performed using the DreamTaq Green PCR kit (Thermo Scientific, UK) on
730 a ProFlex PCR system (Thermo Scientific, UK). PCR reaction conditions were as
731 follows: 3 minutes at 95ºC; 40 cycles of 30 s at 95ºC, 30 s at 68ºC, 90 s at 72ºC; 15
732 minutes at 72ºC.
733

734 Delayed chlorophyll fluorescence and prompt chlorophyll *a*
735 fluorescence imaging

736 Leaf samples were taken from the upper half of the first true leaf of 16-day old
737 seedlings (non-vernalised) grown and entrained in Conviron growth cabinets and were
738 cut into 3 mm by 3 mm pieces and placed on solid 0.8% (w/v) bactoagar, 0.5 x MS
739 Vitamin medium (M3900, Sigma-Aldrich, UK) supplemented with 0.5 µM benzyl-
740 aminopurine (BAP), poured in a black 96 well imaging plates (Greiner, UK). Delayed
741 fluorescence (Gould *et al.* 2009) was measured for 60 s in an LB985 Nightshade
742 (Berthold, UK) camera. Between measurements of DF light was supplied from blue
743 (470 nm) red (660 nm) and LED arrays at 100 µmol m^{-2} s^{-1} during the experiment.
744 Temperature was maintained at 20ºC.
745

746 Chlorophyll *a* fluorescence and calculations of parameters were carried out using a
747 CFimager (Technologica Ltd, Colchester, UK) and the image processing scripts
748 provided by the manufacturer. Chlorophyll fluorescence images were captured using
749 a Stingray F145B ASG camera (Allied Vision Technologies, UK) through an RG665
750 long pass filter to exclude blue light from the LEDs. When imaging under continuous
751 light, leaf fragments were exposed to 40 minutes of 100 µmol m^{-2} s^{-1} of blue light
752 followed by a saturating pulse of 6172 µmol m^{-2} s^{-1} blue light for 800 ms then 20
753 minutes of darkness (with non-actinic measuring light on) followed by a second
754 saturating pulse of 6172 µmol m^{-2} s^{-1} for 800 ms.
755
756 Circadian measures of amplitude, phase, period and relative amplitude error were
757 calculated using the FFT-NLLS method in Biodare2 (www.biodare2.ed.ac.uk)
758 (Zielinski *et al.* 2014). Where necessary data was normalised to between -1 and 1
759 using the normalisation feature of Biodare2.
760

761 Heading date measurements in *TtELF3* kronos lines

762 Seeds sown as described above and moved to long day conditions (Conviron growth
763 cabinet, 16 h light: 8 h dark; 400 µmol m^{-2} s^{-1}, 22°C). After two weeks seedlings
764 transplanted to 10 cm pots. Heading (GS55) was scored once per day.
765

766 Direct contact leaf temperature measurements

767 Leaf surface temperature relative to background temperature was measured using an
768 in-house built device and provides an alternative measure of circadian rhythms caused
769 by circadian regulated changes in the stomatal aperture (Dakhiya and Green 2019).

770 The temperature logger was validated by measuring circadian rhythms of “in-phase”
771 and “anti-phase” wheat leaves where peak temperature, and therefore maximum
772 closure, occurred during the subjective night (Supplemental Figure S15). Leaf
773 temperature measurements were taken from fully expanded flag leaf of 4-week-old
774 plants under continuous light and temperature (200 µmol m^{-2} s^{-1}, 20°C) that were
775 previously grown under long days (16h L: 8h D; 200 µmol m^{-2} s^{-1}, 20°C day: 15°C night)
776 in a growth cabinet (Conviron, UK).
777
778 Wheat was grown in 10 cm pots. Circadian measurements of leaf temperature were
779 taken when the pants were four-weeks old. Type-K thermocouples were attached to
780 the leaf such the end of the thermocouple was pressing onto the surface of the fully
781 expanded flag leaf. This was kept in position by positioning a paperclip onto the leaf
782 and fixing the paperclip to a stake. The thermocouples were connected to an Arduino
783 Mega using the Adafruit 1778, a 10-bit D-A converter and x20 amplifier giving a
784 resolution of ± 0.1°C with a DS3231 RTC added to keep time, temperature was logged
785 every 30 s. Background temperature was measured using unattached thermocouples.
786 Leaf temperatures were averaged using a 60-point moving average, background
787 temperature was then subtracted from leaf temperature to give leaf temperature
788 relative to background.
789

790 **Acknowledgements and Funding**

791 LW, GS and LT were supported by BBSRC
792 studentships BB/K011790/1, BB/M015416/1 and BB/M011194/1 awarded to MAH
793 and AARW, GS is currently supported by UKRI BBSRC grant BB/S006370/1 awarded

to AARW. DCR is supported by UKRI BBSRC grant BB/S002251/1 and GP-C is supported by UKRI BBSRC grant BB/W001209/1, both awarded to AARW.

Contributions

AARW, MAH, AG, KG, LW and GS conceived this study and planned the experiments. LW, GS and LJT performed the experiments and analysed data. DCR and GP-C assisted with scoring heading date and sampling for qRT-PCR. AARW, LW and GS wrote the first draft of the manuscript. AARW, MAH, KG, LW, GS and LJT contributed to the revision of the manuscript.

819 # Bibliography

820 Aguilar, M. and Prieto, P., 2020. Sequence analysis of wheat subtelomeres reveals a
821 high polymorphism among homoeologous chromosomes. *The Plant Genome*,
822 13 (3), e20065.

823 Alvarez, M.A., Tranquilli, G., Lewis, S., Kippes, N., and Dubcovsky, J., 2016. Genetic
824 and physical mapping of the earliness per se locus Eps-A m 1 in Triticum
825 monococcum identifies EARLY FLOWERING 3 (ELF3) as a candidate gene.
826 *Functional & Integrative Genomics*, 16 (4), 365–82.

827 Beales, J., Turner, A., Griffiths, S., Snape, J.W., and Laurie, D.A., 2007. A Pseudo-
828 Response Regulator is misexpressed in the photoperiod insensitive Ppd-D1a
829 mutant of wheat (Triticum aestivum L.). *Theoretical and Applied Genetics*, 115
830 (5), 721–733.

831 Bentley, A.R., Horsnell, R., Werner, C.P., Turner, A.S., Rose, G.A., Bedard, C.,
832 Howell, P., Wilhelm, E.P., Mackay, I.J., Howells, R.M., Greenland, A., Laurie,
833 D.A., and Gosman, N., 2013. Short, natural, and extended photoperiod
834 response in BC2F4 lines of bread wheat with different Photoperiod-1 (Ppd-1)
835 alleles. *Journal of Experimental Botany*, 64 (7), 1783–1793.

836 Boden, S.A., Weiss, D., Ross, J.J., Davies, N.W., Trevaskis, B., Chandler, P.M., and
837 Swain, S.M., 2014. EARLY FLOWERING3 Regulates Flowering in Spring Barley
838 by Mediating Gibberellin Production and FLOWERING LOCUS T Expression.
839 *The Plant Cell*, 26 (4), 1557–1569.

840 Bouché, F., Woods, D.P., Linden, J., Li, W., Mayer, K.S., Amasino, R.M., and
841 Périlleux, C., 2022. EARLY FLOWERING 3 and Photoperiod Sensing in
842 Brachypodium distachyon. *Frontiers in Plant Science*, 12 (January), 1–14.

843 Brinton, J., Ramirez-Gonzalez, R.H., Simmonds, J., Wingen, L., Orford, S., Griffiths,

844 S., Haberer, G., Spannagl, M., Walkowiak, S., Pozniak, C., and Uauy, C., 2020.
845 A haplotype-led approach to increase the precision of wheat breeding.
846 *Communications Biology*, 3 (1), 1–11.
847 Calixto, C.P.G., Waugh, R., and Brown, J.W.S., 2015. Evolutionary Relationships
848 Among Barley and Arabidopsis Core Circadian Clock and Clock-Associated
849 Genes. *Journal of Molecular Evolution*, 80 (2), 108–119.
850 Camargo, A. V., Mott, R., Gardner, K.A., Mackay, I.J., Corke, F., Doonan, J.H., Kim,
851 J.T., and Bentley, A.R., 2016. Determining Phenological Patterns Associated
852 with the Onset of Senescence in a Wheat MAGIC Mapping Population. *Frontiers*
853 *in Plant Science*, 7, 1540.
854 Campoli, C., Pankin, A., Drosse, B., Casao, C.M., Davis, S.J., and Von Korff, M.,
855 2013. HvLUX1 is a candidate gene underlying the early maturity 10 locus in
856 barley: Phylogeny, diversity, and interactions with the circadian clock and
857 photoperiodic pathways. *New Phytologist*, 199 (4), 1045–1059.
858 Chen, A., Li, C., Hu, W., Lau, M.Y., Lin, H., Rockwell, N.C., Martin, S.S., Jernstedt, J.
859 a, Lagarias, J.C., and Dubcovsky, J., 2014. PHYTOCHROME C plays a major
860 role in the acceleration of wheat flowering under long-day photoperiod.
861 *Proceedings of the National Academy of Sciences of the United States of*
862 *America*, 111 (28), 10037–10044.
863 Clavijo, B.J., Venturini, L., Schudoma, C., Accinelli, G.G., Kaithakottil, G., Wright, J.,
864 Borrill, P., Kettleborough, G., Heavens, D., Chapman, H., Lipscombe, J., Barker,
865 T., Lu, F.H., McKenzie, N., Raats, D., Ramirez-Gonzalez, R.H., Coince, A.,
866 Peel, N., Percival-Alwyn, L., Duncan, O., Trösch, J., Yu, G., Bolser, D.M.,
867 Namaati, G., Kerhornou, A., Spannagl, M., Gundlach, H., Haberer, G., Davey,
868 R.P., Fosker, C., Di Palma, F., Phillips, A.L., Millar, A.H., Kersey, P.J., Uauy, C.,

869 Krasileva, K. V., Swarbreck, D., Bevan, M.W., and Clark, M.D., 2017. An
870 improved assembly and annotation of the allohexaploid wheat genome identifies
871 complete families of agronomic genes and provides genomic evidence for
872 chromosomal translocations. *Genome Research*, 27 (5), 885–896.
873 Cockram, J., Jones, H., Leigh, F.J., O'Sullivan, D., Powell, W., Laurie, D.A., and
874 Greenland, A.J., 2007. Control of flowering time in temperate cereals: genes,
875 domestication, and sustainable productivity. *Journal of Experimental Botany*, 58
876 (6), 1231–1244.
877 Dakhiya, Y. and Green, R.M., 2019. Thermal imaging as a non-invasive technique
878 for analyzing circadian rhythms in plants. *New Phytologist*, 224, 1685–1696.
879 Dakhiya, Y., Hussien, D., Fridman, E., Kiflawi, M., and Green, R., 2017. Correlations
880 between Circadian Rhythms and Growth in Challenging Environments. *Plant*
881 *Physiology*, 173 (3), 1724–1734.
882 Dixon, L.E., Knox, K., Kozma-Bognar, L., Southern, M.M., Pokhilko, A., and Millar,
883 A.J., 2011. Temporal repression of core circadian genes is mediated through
884 EARLY FLOWERING 3 in Arabidopsis. *Current Biology*, 21 (2), 120–125.
885 Dodd, A.N., Salathia, N., Hall, A., Kévei, E., Tóth, R., Nagy, F., Hibberd, J.M., Millar,
886 A.J., and Webb, A. a R., 2005. Plant circadian clocks increase photosynthesis,
887 growth, survival, and competitive advantage. *Science (New York, N.Y.)*, 309
888 (5734), 630–633.
889 Ezer, D., Jung, J.H., Lan, H., Biswas, S., Gregoire, L., Box, M.S., Charoensawan, V.,
890 Cortijo, S., Lai, X., Stöckle, D., Zubieta, C., Jaeger, K.E., and Wigge, P.A., 2017.
891 The evening complex coordinates environmental and endogenous signals in
892 Arabidopsis. *Nature Plants*, 3 (7).
893 Faricelli, M.E., Valárik, M., and Dubcovsky, J., 2010. Control of flowering time and

894 spike development in cereals: The earliness per se Eps-1 region in wheat, rice,
895 and Brachypodium. *Functional and Integrative Genomics*, 10 (2), 293–306.
896 Faure, S., Turner, a. S., Gruszka, D., Christodoulou, V., Davis, S.J., von Korff, M.,
897 and Laurie, D. a., 2012. Mutation at the circadian clock gene EARLY
898 MATURITY 8 adapts domesticated barley (Hordeum vulgare) to short growing
899 seasons. *Proceedings of the National Academy of Sciences*, 109 (21), 8328–
900 8333.
901 Gao, M., Geng, F., Klose, C., Staudt, A.-M., Huang, H., Nguyen, D., Lan, H.,
902 Mockler, T.C., Nusinow, D.A., Hiltbrunner, A., Schäfer, E., Wigge, P.A., and
903 Jaeger, K.E., 2019. Phytochromes measure photoperiod in Brachypodium.
904 *bioRxiv*.
905 Gardner, K.A., Wittern, L.M., and Mackay, I.J., 2016. A highly recombined, high-
906 density, eight-founder wheat MAGIC map reveals extensive segregation
907 distortion and genomic locations of introgression segments. *Plant Biotechnology*
908 *Journal*, 14 (6), 1406–1417.
909 Gawronski, P., Ariyadasa, R., Himmelbach, A., Poursarebani, N., Kilian, B., Stein,
910 N., Steuernagel, B., Hensel, G., Kumlehn, J., Sehgal, S.K., Gill, B.S., Gould, P.,
911 Hall, A., and Schnurbusch, T., 2014. A Distorted Circadian Clock Causes Early
912 Flowering and Temperature-Dependent Variation in Spike Development in the
913 Eps-3Am Mutant of Einkorn Wheat. *Genetics*, 196 (4), 1253–1261.
914 Gerland, P., Raftery, A.E., Sevcikova, H., Li, N., Gu, D., Spoorenberg, T., Alkema,
915 L., Fosdick, B.K., Chunn, J., Lalic, N., Bay, G., Buettner, T., Heilig, G.K., and
916 Wilmoth, J., 2014. World population stabilization unlikely this century. *Science*,
917 346 (6206), 234–237.
918 Gilmour, A.R., Cullis, B.R., and Verbyla, A.P., 1997. Accounting for Natural and

919 Extraneous Variation in the Analysis of Field Experiments. *Journal of*
920 *Agricultural, Biological, and Environmental Statistics*, 2 (3), 269–293.
921 Gould, P.D., Diaz, P., Hogben, C., Kusakina, J., Salem, R., Hartwell, J., and Hall, A.,
922 2009. Delayed fluorescence as a universal tool for the measurement of
923 circadian rhythms in higher plants. *Plant Journal*, 58 (5), 893–901.
924 Griffiths, S., Simmonds, J., Leverington, M., Wang, Y., Fish, L., Sayers, L., Alibert,
925 L., Orford, S., Wingen, L., Herry, L., Faure, S., Laurie, D., Bilham, L., and
926 Snape, J., 2009. Meta-QTL analysis of the genetic control of ear emergence in
927 elite European winter wheat germplasm. *Theoretical and Applied Genetics*, 119
928 (3), 383–395.
929 Guo, W., Xin, M., Wang, Z., Yao, Y., Hu, Z., Song, W., Yu, K., Chen, Y., Wang, X.,
930 Guan, P., Appels, R., Peng, H., Ni, Z., and Sun, Q., 2020. Origin and adaptation
931 to high altitude of Tibetan semi-wild wheat. *Nature Communications*, 11 (1), 1–
932 12.
933 Harmer, S.L. and Kay, S.A., 2005. Positive and negative factors confer phase-
934 specific circadian regulation of transcription in Arabidopsis. *Plant Cell*, 17 (7),
935 1926–1940.
936 Hawkesford, M.J., Araus, J.L., Park, R., Calderini, D., Miralles, D., Shen, T., Zhang,
937 J., and Parry, M. a. J., 2013. Prospects of Doubling Global Wheat Yields. *Food*
938 *and Energy Security*, 2 (1), 34–48.
939 He, F., Pasam, R., Shi, F., Kant, S., Keeble-Gagnère, G., Kay, P., Forrest, K., Fritz,
940 A., Hucl, P., Wiebe, K., Know, R., Cuthbert, R., Pozniak, C., Akhunova, A.,
941 Morrell, P.L., Davies, J.P., Webb, S.R., Spangenberg, G., Hayes, B., Daetwyler,
942 H., Tibbits, J., Hayden, M., and Akhunov, E., 2019. Exome sequencing
943 highlights the role of wild-relative introgression in shaping the adaptive

944 landscape of the wheat genome. *Nature genetics*, 51 (5), 896–904.
945 Herrero, E., Kolmos, E., Bujdoso, N., Yuan, Y., Wang, M., Berns, M.C., Uhlworm, H.,
946 Coupland, G., Saini, R., Jaskolski, M., Webb, A., Goncalves, J., and Davis, S.J.,
947 2012. EARLY FLOWERING4 Recruitment of EARLY FLOWERING3 in the
948 Nucleus Sustains the Arabidopsis Circadian Clock. *the Plant Cell Online*, 24 (2),
949 428–443.
950 Hsu, P.Y. and Harmer, S.L., 2014. Wheels within wheels: The plant circadian
951 system. *Trends in Plant Science*, 19 (4), 240–249.
952 Huang, B.E. and George, A.W., 2011. R/mpMap: A computational platform for the
953 genetic analysis of multiparent recombinant inbred lines. *Bioinformatics*, 27 (5),
954 727–729.
955 Huang, H., Alvarez, S., Bindbeutel, R., Shen, Z., Naldrett, M.J., Evans, B.S., Briggs,
956 S.P., Hicks, L.M., Kay, S.A., and Nusinow, D.A., 2016. Identification of evening
957 complex associated proteins in arabidopsis by affinity purification and mass
958 spectrometry. *Molecular and Cellular Proteomics*, 15 (1), 201–217.
959 Huang, H., Gehan, M.A., Huss, S.E., Alvarez, S., Lizarraga, C., Gruebbling, E.L.,
960 Gierer, J., Naldrett, M.J., Bindbeutel, R.K., Evans, B.S., Mockler, T.C., and
961 Nusinow, D.A., 2017. Cross-species complementation reveals conserved
962 functions for EARLY FLOWERING 3 between monocots and dicots. *Plant
963 Direct*, 00, 1–14.
964 Hyles, J., Vautrin, S., Pettolino, F., MacMillan, C., Stachurski, Z., Breen, J., Berges,
965 H., Wicker, T., and Spielmeyer, W., 2017. Repeat-length variation in a wheat
966 cellulose synthase-like gene is associated with altered tiller number and stem
967 cell wall composition. *Journal of Experimental Botany*, 68 (7), 1519–1529.
968 Jordan, K.W., Wang, S., Lun, Y., Gardiner, L.-J., MacLachlan, R., Hucl, P., Wiebe,

969 K., Wong, D., Forrest, K.L., Sharpe, A.G., Sidebottom, C.H., Hall, N., Toomajian,
970 C., Close, T., Dubcovsky, J., Akhunova, A., Talbert, L., Bansal, U.K., Bariana,
971 H.S., Hayden, M.J., Pozniak, C., Jeddeloh, J.A., Hall, A., and Akhunov, E.,
972 2015. A haplotype map of allohexaploid wheat reveals distinct patterns of
973 selection on homoeologous genomes. *Genome Biology*, 16 (1), 48.
974 Kippes, N., VanGessel, C., Hamilton, J., Akpinar, A., Budak, H., Dubcovsky, J.,
975 Dubcovsky, J., and Pearce, S., 2020. Effect of phyB and phyC loss-of-function
976 mutations on the wheat transcriptome under short and long day photoperiods.
977 *BMC Plant Biology*, 20 (1), 1–17.
978 Kolmos, E., Nowak, M., Werner, M., Fischer, K., Schwarz, G., Mathews, S., Schoof,
979 H., Nagy, F., Bujnicki, J.M., and Davis, S.J., 2009. Integrating ELF4 into the
980 circadian system through combined structural and functional studies. *HFSP*
981 *Journal*, 3 (5), 350–366.
982 Krasileva, K. V, Vasquez-gross, H.A., Howell, T., Bailey, P., Paraiso, F., and
983 Clissold, L., 2017. Uncovering hidden variation in polyploid wheat. *PNAS*, E913–
984 E921.
985 Lai, X., Bendix, C., Yan, L., Zhang, Y., Schnable, J.C., and Harmon, F.G., 2020.
986 Interspecific analysis of diurnal gene regulation in panicoid grasses identifies
987 known and novel regulatory motifs. *BMC genomics*, 21 (1), 428.
988 Langer, S.M., Longin, C.F.H., and Würschum, T., 2014. Flowering time control in
989 European winter wheat. *Frontiers in Plant Science*, 5 (OCT), 1–11.
990 Lundqvist, U., 2014. Scandinavian mutation research in barley - a historical review.
991 *Hereditas*, 151 (6), 123–131.
992 Mackay, I.J., Bansept-Basler, P., Bentley, A.R., Cockram, J., Gosman, N.,
993 Greenland, A.J., Horsnell, R., Howells, R., O'Sullivan, D.M., Rose, G.A., and

994 Howell, P.J., 2014. An eight-parent multiparent advanced generation inter-cross
995 population for winter-sown wheat: Creation, properties, and validation. *G3:*
996 *Genes, Genomes, Genetics*, 4 (9), 1603–1610.
997 Matsubara, K., Ogiso-Tanaka, E., Hori, K., Ebana, K., Ando, T., and Yano, M., 2012.
998 Natural variation in Hd17, a homolog of arabidopsis ELF3 that is involved in rice
999 photoperiodic flowering. *Plant and Cell Physiology*, 53 (4), 709–716.
1000 McClung, C., 2019. The Plant Circadian Oscillator. *Biology*, 8 (1), 14.
1001 Michael, T.P., Mockler, T.C., Breton, G., McEntee, C., Byer, A., Trout, J.D., Hazen,
1002 S.P., Shen, R., Priest, H.D., Sullivan, C.M., Givan, S.A., Yanovsky, M., Hong, F.,
1003 Kay, S.A., and Chory, J., 2008. Network discovery pipeline elucidates conserved
1004 time-of-day-specific cis-regulatory modules. *PLoS Genetics*, 4 (2), 14.
1005 Mizuno, N., Kinoshita, M., Kinoshita, S., Nishida, H., Fujita, M., Kato, K., Murai, K.,
1006 and Nasuda, S., 2016. Loss-of-function mutations in three homoeologous
1007 PHYTOCLOCK 1 genes in common wheat are associated with the extra-early
1008 flowering phenotype. *PLoS ONE*, 11 (10), 1–19.
1009 Mizuno, N., Nitta, M., Sato, K., and Nasuda, S., 2012. A wheat homologue of
1010 PHYTOCLOCK 1 is a candidate gene conferring the early heading phenotype to
1011 einkorn wheat. *Genes & genetic systems*, 87 (6), 357–67.
1012 Nagel, D.H. and Kay, S.A., 2012. Complexity in the wiring and regulation of plant
1013 circadian networks. *Current Biology*, 22 (16), 648–657.
1014 Nusinow, D.A., Helfer, A., Hamilton, E.E., King, J.J., Imaizumi, T., Schultz, T.F.,
1015 Farré, E.M., and Kay, S.A., 2011. The ELF4–ELF3–LUX complex links the
1016 circadian clock to diurnal control of hypocotyl growth. *Nature*, 475 (7356), 398–
1017 402.
1018 Ochagavía, H., Prieto, P., Zikhali, M., Griffiths, S., and Slafer, G.A., 2019. Earliness

1019 Per Se by Temperature Interaction on Wheat Development. *Scientific Reports*, 9
1020 (1), 2584.
1021 Paradis, E. and Schliep, K., 2019. ape 5.0: an environment for modern phylogenetics
1022 and evolutionary analyses in R. *Bioinformatics*, 35 (3), 526–528.
1023 Pearce, S., Kippes, N., Chen, A., Debernardi, J.M., and Dubcovsky, J., 2016. RNA-
1024 seq studies using wheat PHYTOCHROME B and PHYTOCHROME C mutants
1025 reveal shared and specific functions in the regulation of flowering and shade-
1026 avoidance pathways. *BMC Plant Biology*, 16 (1), 1–19.
1027 Pearce, S., Shaw, L.M., Lin, H., Cotter, J.D., Li, C., and Dubcovsky, J., 2017. Night-
1028 break experiments shed light on the Photoperiod 1-mediated flowering. *Plant*
1029 *Physiology*, pp.00361.2017.
1030 Przewieslik-Allen, A.M., Wilkinson, P.A., Burridge, A.J., Winfield, M.O., Dai, X.,
1031 Beaumont, M., King, J., Yang, C., Griffiths, S., Wingen, L.U., Horsnell, R.,
1032 Bentley, A.R., Shewry, P., Barker, G.L.A., and Edwards, K.J., 2021. The role of
1033 gene flow and chromosomal instability in shaping the bread wheat genome.
1034 *Nature Plants*, 7 (2), 172–183.
1035 Scott, M.F., Fradgley, N., Bentley, A.R., Brabbs, T., Corke, F., Gardner, K.A.,
1036 Horsnell, R., Howell, P., Ladejobi, O., Mackay, I.J., Mott, R., and Cockram, J.,
1037 2021. Limited haplotype diversity underlies polygenic trait architecture across 70
1038 years of wheat breeding. *Genome Biology*, 22 (1), 1–30.
1039 Scutari, M., Howell, P., Balding, D.J., and Mackay, I., 2014. Multiple Quantitative
1040 Trait Analysis Using Bayesian Networks. *Genetics*, 198 (1), 129–137.
1041 Shah, R., 2013. mpMapinteractive: Interactive components for package mpMap. R
1042 package version 0.2.
1043 Shaw, L.M., Li, C., Woods, D.P., Alvarez, M.A., Lin, H., Lau, M.Y., Chen, A., and

1044 Dubcovsky, J., 2020. Epistatic interactions between PHOTOPERIOD1,
1045 CONSTANS1 and CONSTANS2 modulate the photoperiodic response in wheat.
1046 *PLoS Genetics*, 16 (7), 1–28.
1047 Shaw, L.M., Turner, A.S., and Laurie, D.A., 2012. The impact of photoperiod
1048 insensitive Ppd-1a mutations on the photoperiod pathway across the three
1049 genomes of hexaploid wheat (Triticum aestivum). *The Plant Journal*, 71 (1), 71–
1050 84.
1051 Steed, G., Cano-Ramirez, D.L., Hannah, M.A., and Webb, A.A., 2021.
1052 Chronoculture, harnessing the circadian clock to improve crop yield and
1053 sustainability. *Science*, 372 (April).
1054 Sun, H., Zhang, W., Wu, Y., Gao, L., Cui, F., Zhao, C., Guo, Z., and Jia, J., 2020.
1055 The Circadian Clock Gene, TaPRR1, Is Associated With Yield-Related Traits in
1056 Wheat (Triticum aestivum L.). *Frontiers in Plant Science*, 11, 285.
1057 Sun, L., Yang, W., Li, Y., Shan, Q., Ye, X., Wang, D., Yu, K., Lu, W., Xin, P., Pei, Z.,
1058 Guo, X., Liu, D., Sun, J., Zhan, K., Chu, J., and Zhang, A., 2019. A wheat
1059 dominant dwarfing line with Rht12 , which reduces stem cell length and affects
1060 gibberellic acid synthesis, is a 5AL terminal deletion line. *The Plant Journal*, 97
1061 (5), 887–900.
1062 Turner, A.S., Faure, S., Zhang, Y., and Laurie, D.A., 2013. The effect of day-neutral
1063 mutations in barley and wheat on the interaction between photoperiod and
1064 vernalization. *Theoretical and Applied Genetics*, 126 (9), 2267–2277.
1065 Vandesompele, J., De Preter, K., Pattyn, F., Poppe, B., Van Roy, N., De Paepe, A.,
1066 and Speleman, F., 2002. Accurate normalization of real-time quantitative RT-
1067 PCR data by geometric averaging of multiple internal control genes. *Genome*
1068 *biology*, 3 (7), RESEARCH0034.

1069 Verbyla, A.P., George, A.W., Cavanagh, C.R., and Verbyla, K.L., 2014.
1070 Whole-genome QTL analysis for MAGIC. *Theoretical and Applied Genetics*, 127
1071 (8), 1753–1770.
1072 Walkowiak, S., Gao, L., Monat, C., Haberer, G., Kassa, M.T., Brinton, J., Ramirez-
1073 Gonzalez, R.H., Kolodziej, M.C., Delorean, E., Thambugala, D., Klymiuk, V.,
1074 Byrns, B., Gundlach, H., Bandi, V., Siri, J.N., Nilsen, K., Aquino, C.,
1075 Himmelbach, A., Copetti, D., Ban, T., Venturini, L., Bevan, M., Clavijo, B., Koo,
1076 D.H., Ens, J., Wiebe, K., N'Diaye, A., Fritz, A.K., Gutwin, C., Fiebig, A., Fosker,
1077 C., Fu, B.X., Accinelli, G.G., Gardner, K.A., Fradgley, N., Gutierrez-Gonzalez, J.,
1078 Halstead-Nussloch, G., Hatakeyama, M., Koh, C.S., Deek, J., Costamagna,
1079 A.C., Fobert, P., Heavens, D., Kanamori, H., Kawaura, K., Kobayashi, F.,
1080 Krasileva, K., Kuo, T., McKenzie, N., Murata, K., Nabeka, Y., Paape, T.,
1081 Padmarasu, S., Percival-Alwyn, L., Kagale, S., Scholz, U., Sese, J., Juliana, P.,
1082 Singh, R., Shimizu-Inatsugi, R., Swarbreck, D., Cockram, J., Budak, H.,
1083 Tameshige, T., Tanaka, T., Tsuji, H., Wright, J., Wu, J., Steuernagel, B., Small,
1084 I., Cloutier, S., Keeble-Gagnère, G., Muehlbauer, G., Tibbets, J., Nasuda, S.,
1085 Melonek, J., Hucl, P.J., Sharpe, A.G., Clark, M., Legg, E., Bharti, A., Langridge,
1086 P., Hall, A., Uauy, C., Mascher, M., Krattinger, S.G., Handa, H., Shimizu, K.K.,
1087 Distelfeld, A., Chalmers, K., Keller, B., Mayer, K.F.X., Poland, J., Stein, N.,
1088 McCartney, C.A., Spannagl, M., Wicker, T., and Pozniak, C.J., 2020. Multiple
1089 wheat genomes reveal global variation in modern breeding. *Nature*, 588 (7837),
1090 277–283.
1091 Wang, J., Wen, W., Hanif, M., Xia, X., Wang, H., Liu, S., Liu, J., Yang, L., Cao, S.,
1092 and He, Z., 2016. TaELF3-1DL, a homolog of ELF3, is associated with heading
1093 date in bread wheat. *Molecular Breeding*, 36 (12), 1–9.

1094 Weller, J.L., Liew, L.C., Hecht, V.F.G., Rajandran, V., Laurie, R.E., Ridge, S.,
1095 Wenden, B., Schoor, J.K.V., Jaminon, O., Blassiau, C., Dalmais, M., Rameau,
1096 C., Bendahmane, A., Macknight, R.C., and Lejeune-Hénaut, I., 2012. A
1097 conserved molecular basis for photoperiod adaptation in two temperate
1098 legumes. *Proceedings of the National Academy of Sciences of the United States*
1099 *of America*, 109 (51), 21158–21163.
1100 Wilkinson, P.A., Winfield, M.O., Barker, G.L.A., Allen, A.M., Burridge, A., Coghill,
1101 J.A., and Edwards, K.J., 2012. CerealsDB 2.0: an integrated resource for plant
1102 breeders and scientists. *BMC Bioinformatics*, 13 (1), 219.
1103 Winfield, M.O., Allen, A.M., Burridge, A.J., Barker, G.L.A., Benbow, H.R., Wilkinson,
1104 P.A., Coghill, J., Waterfall, C., Davassi, A., Scopes, G., Pirani, A., Webster, T.,
1105 Brew, F., Bloor, C., King, J., West, C., Griffiths, S., King, I., Bentley, A.R., and
1106 Edwards, K.J., 2016. High-density SNP genotyping array for hexaploid wheat
1107 and its secondary and tertiary gene pool. *Plant Biotechnology Journal*, 14 (5),
1108 1195–1206.
1109 Yao, W., Li, G., Yu, Y., and Ouyang, Y., 2018. funRiceGenes dataset for
1110 comprehensive understanding and application of rice functional genes.
1111 *GigaScience*, 7 (1), 1–9.
1112 Zadoks, J.C., Chang, T.T., and Konzak, C.F., 1974. A decimal code for the growth
1113 stages of cereals. *Weed Research*, 14 (6), 415–421.
1114 Zakhrabekova, S., Gough, S.P., Braumann, I., Muller, A.H., Lundqvist, J., Ahmann,
1115 K., Dockter, C., Matyszczak, I., Kurowska, M., Druka, A., Waugh, R., Graner, A.,
1116 Stein, N., Steuernagel, B., Lundqvist, U., and Hansson, M., 2012. Induced
1117 mutations in circadian clock regulator Mat-a facilitated short-season adaptation
1118 and range extension in cultivated barley. *Proceedings of the National Academy*

1119 *of Sciences*, 109 (11), 4326–4331.
1120 Zhai, H., Jiang, C., Zhao, Y., Yang, S., Li, Y., Yan, K., Wu, S., Luo, B., Du, Y., Jin,
1121 H., Liu, X., Zhang, Y., Lu, F., Reynolds, M., Ou, X., Qiao, W., Jiang, Z., Peng,
1122 T., Gao, D., Hu, W., Wang, J., Gao, H., Yin, G., Zhang, K., Li, G., and Wang, D.,
1123 2021. Wheat heat tolerance is impaired by heightened deletions in the distal end
1124 of 4AL chromosomal arm. *Plant Biotechnology Journal*, 19 (5), 1038–1051.
1125 Zhao, J., Huang, X., Ouyang, X., Chen, W., Du, A., and Zhu, L., 2012. OsELF3-1 ,
1126 an Ortholog of Arabidopsis EARLY FLOWERING 3 , Regulates Rice Circadian
1127 Rhythm and Photoperiodic Flowering. *PLoS ONE*, 7 (8), 1–10.
1128 Zielinski, T., Moore, A.M., Troup, E., Halliday, K.J., and Millar, A.J., 2014. Strengths
1129 and limitations of period estimation methods for circadian data. *PLoS ONE*, 9
1130 (5).
1131 Zikhali, M., Wingen, L.U., and Griffiths, S., 2016. Delimitation of the Earliness per se
1132 D1 (Eps-D1) flowering gene to a subtelomeric chromosomal deletion in bread
1133 wheat (Triticum aestivum). *Journal of Experimental Botany*, 67 (1), 287–299.
1134
1135
1136
1137
1138
1139
1140
1141
1142
1143

1144 # Figures

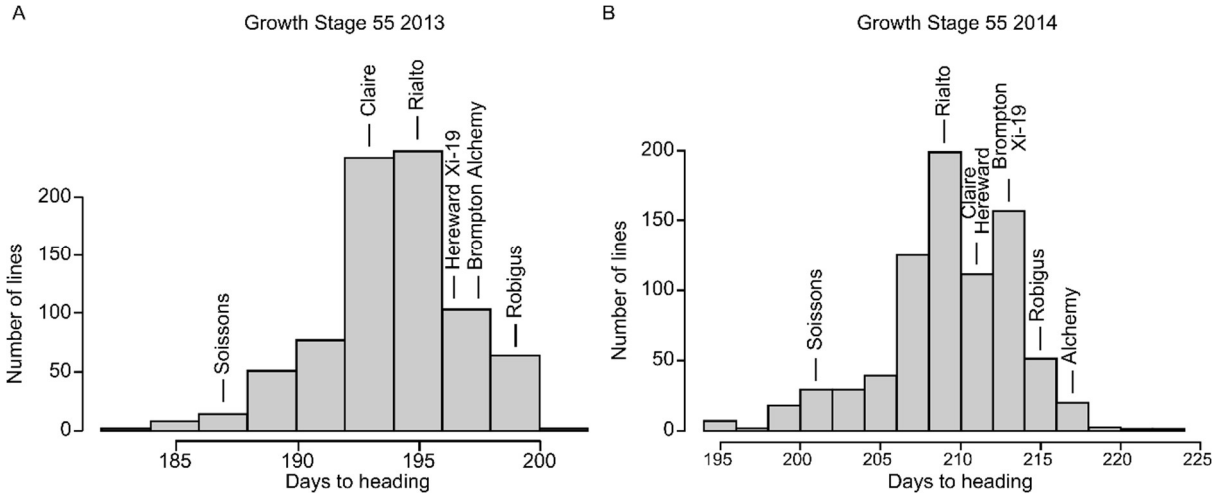

1145

1146 **Figure 1**. **Variation in time to reach GS55 across a UK wheat MAGIC population**.

1147 Time in days for individual MAGIC RILs (recombinant inbred lines) to reach GS55 for the (A) 2012/2013

1148 growing season and (B) 2013/2014 growing season. The number of days after sowing to reach GS55

1149 for the eight MAGIC parents is indicated by arrows.

1150

1151

1152

1153

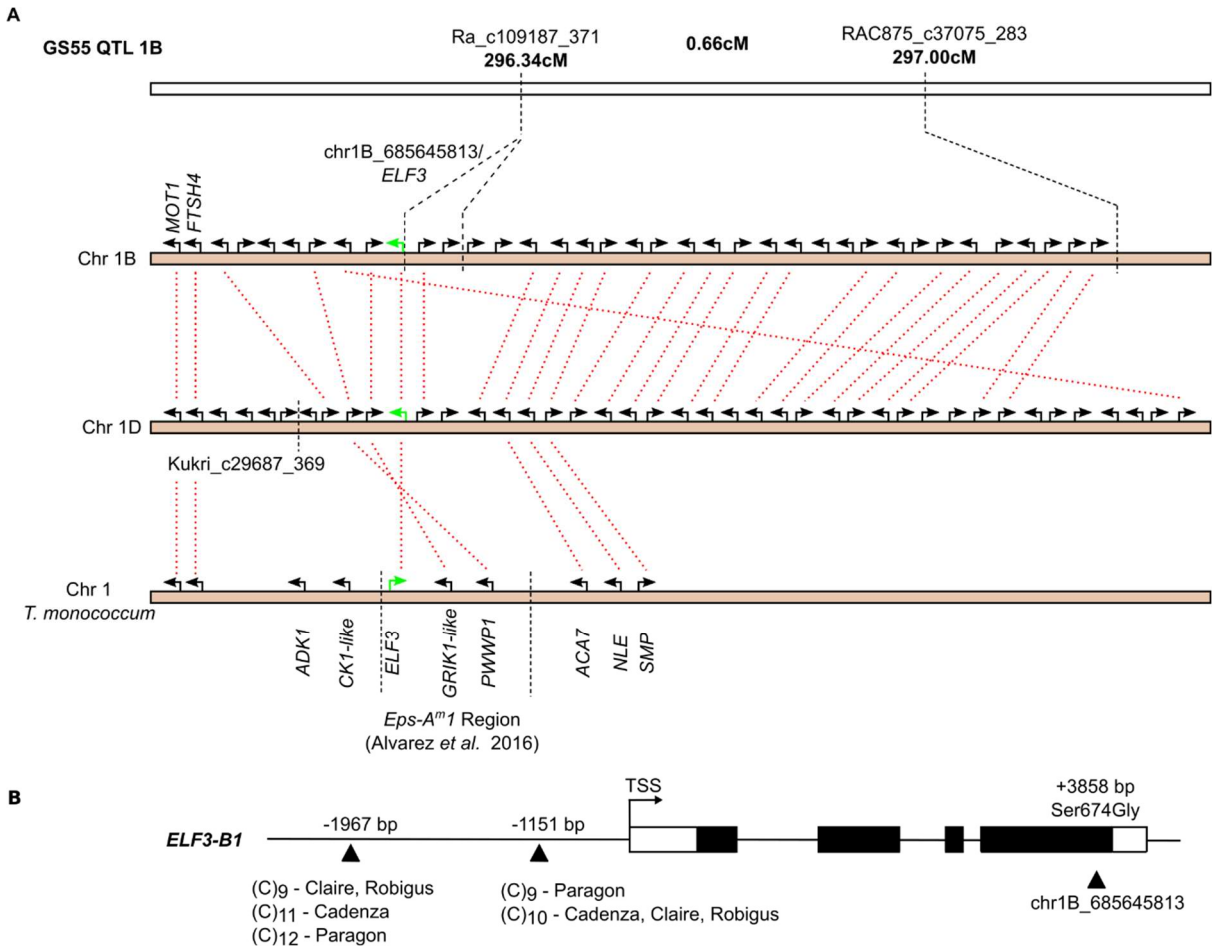

1154

1155

1156 **Figure 2**. ***ELF3* is a candidate gene for *Eps-B1*.**

1157 (A) Syntenic relationships of the *Eps-B1* QTL to the *Eps-D1* QTL and the *T. monococcum Eps-A^{m}1*

1158 QTL. *ELF3* highlighted in green. (B) *TaELF3-B1* gene model with exons represented by filled

1159 rectangles, UTR's as white rectangles. The two promoter cytosine repeat polymorphisms with location

1160 relative to the transcription start site (TSS) are indicated with the cytosine (C) repeat number for Claire,

1161 Robigus, Cadenza and Paragon. The Ser674Gly SNP is situated within exon 4 of *ELF3-B1.*

1162

1163

1164

1165

1166

1167

1168

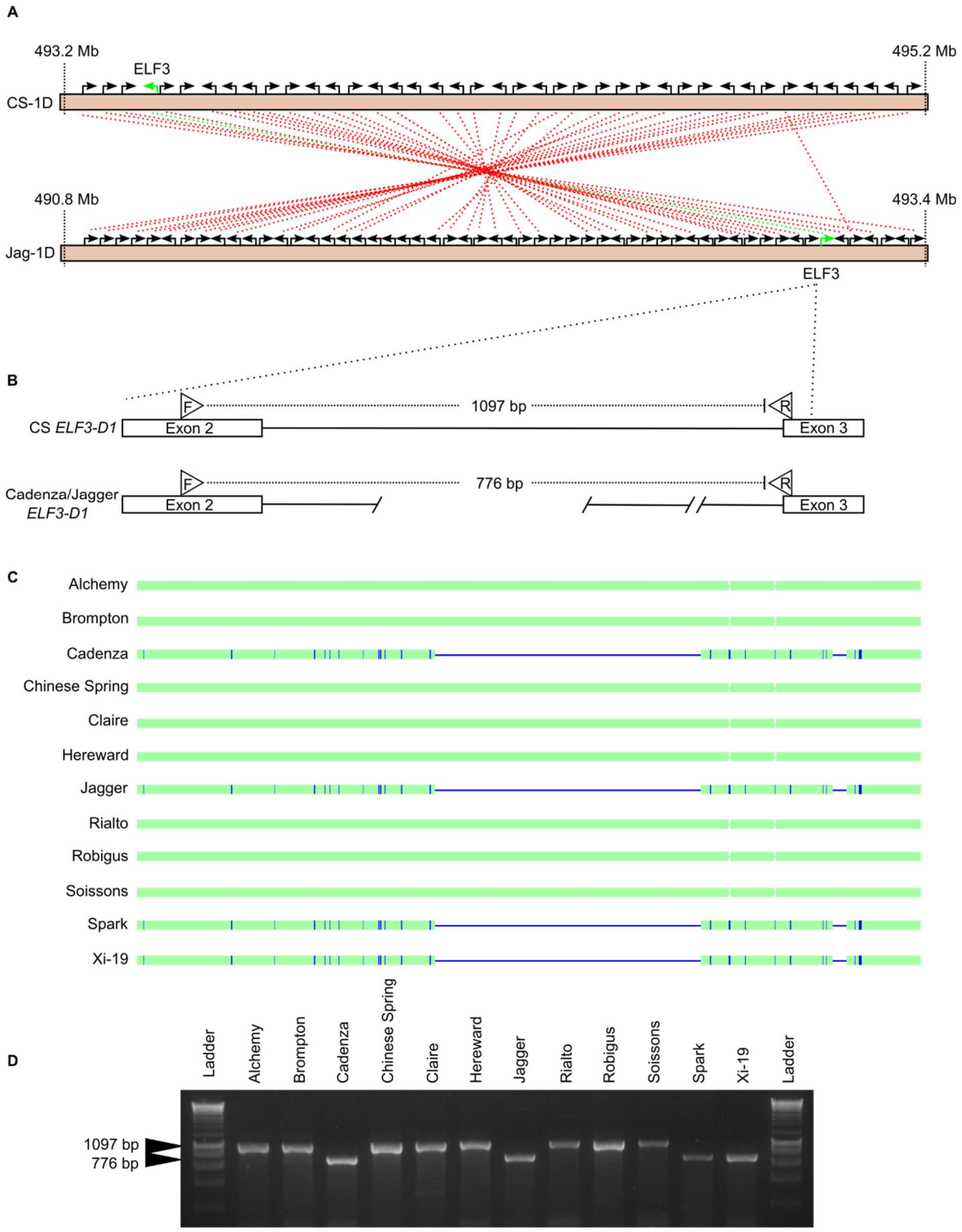

Figure 3. A subtelomeric chromosomal introgression and inversion containing *ELF3-D1* is likely to be the causal polymorphism underlying the *Eps-D1* QTL.

(A) Syntenic relationships between the distal end of Chinese Spring (CS) 1D chromosome (IWGSCv1.1) and Jagger (Jag) 1D (PGSBv2.0), *TaELF3-D1* highlighted in green, each black arrow corresponds to a gene in the forward (pointing right) or reverse (pointing left) strand. (B) the Cadenza/Jagger *ELF3-D1*

1175 contains a deletion within intron 2 which is not present in CS, F and R refer to relative primer binding
1176 sites for PCR amplification shown in (C). (D) Agarose gel separation of PCR products from (C). A PCR
1177 product at 776bp is indicative of the presence of a subtelomeric chromosomal introgression and
1178 inversion.

1179
1180
1181
1182
1183
1184
1185
1186
1187
1188
1189
1190
1191
1192
1193
1194
1195
1196
1197
1198
1199
1200
1201
1202
1203
1204
1205
1206
1207

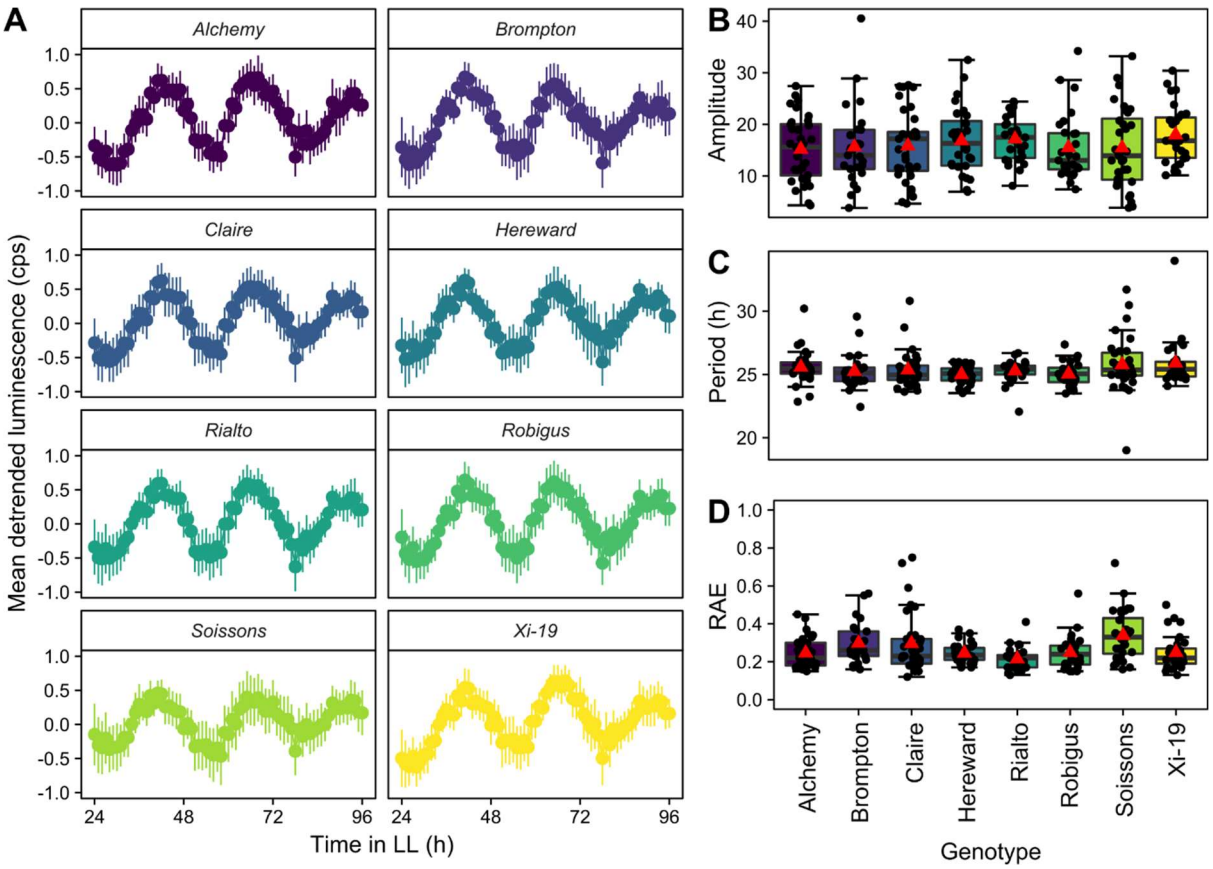

Figure 4. Circadian rhythms of delayed chlorophyll fluorescence in the MAGIC parents. (A) Mean DF luminescence in counts per second (cps) normalised to -1 to 1 using Biodare2 with error bars representing standard deviation (n = 27 - 33). Circadian amplitude (B), period (C) and RAE (D) calculated using FFT-NLLS (Biodare2). Upper and lower hinges represent the first and third quartiles (25th and 75th percentiles), the middle hinge represents the median value, red triangle represents mean value and black dots represent individual replicates.

1226

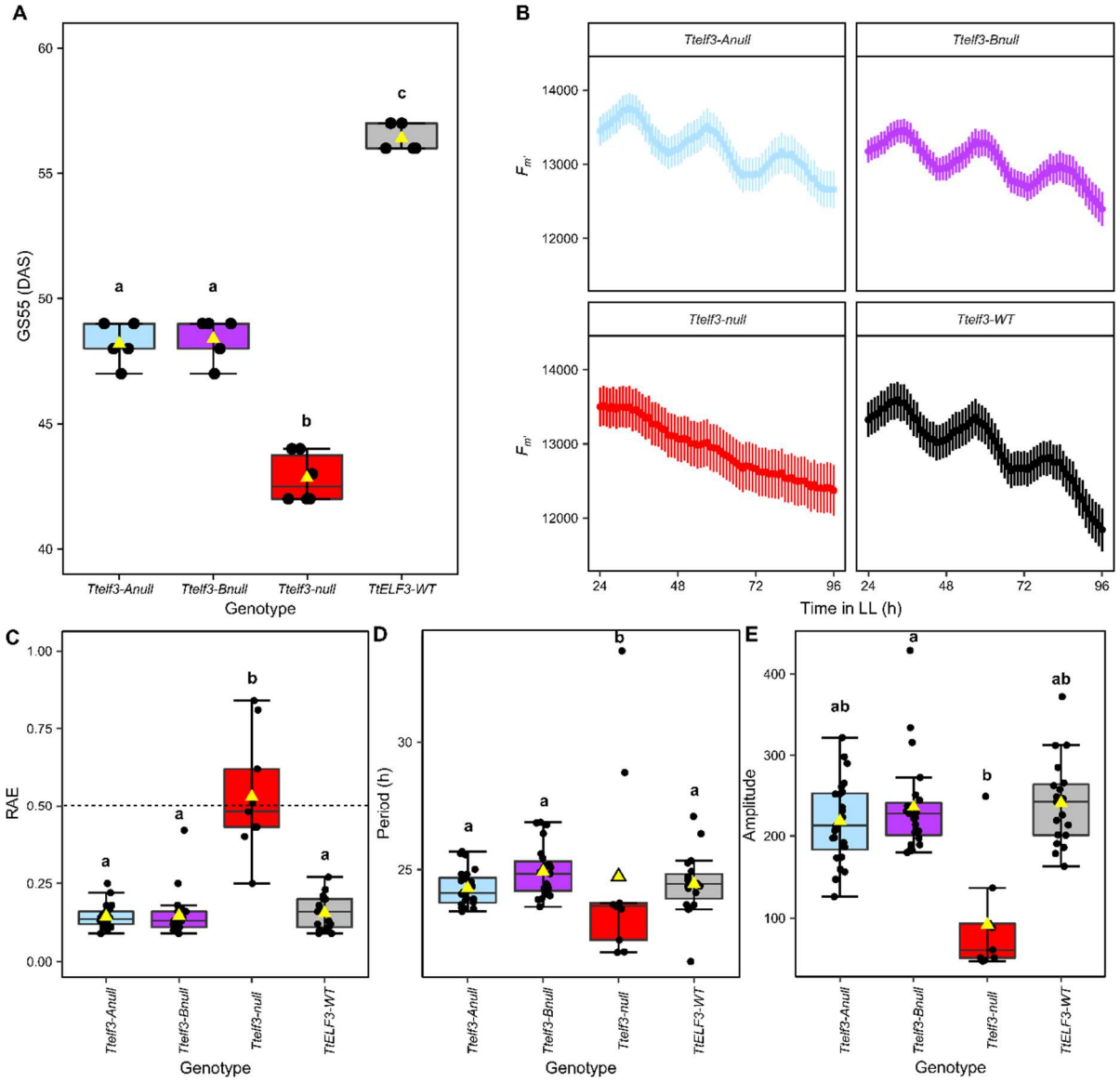

1227

1228 **Figure 5. Mutation of single *ELF3* homoeologues affects heading date but not circadian**
1229 **rhythms of chlorophyll *a* fluorescence but *Ttelf3*-null is arrhythmic in continuous light.**
1230 (A) GS55 for *Ttelf3*-null (red), *Ttelf3*-Anull (blue), *Ttelf3*-Bnull (purple) and *TtELF3*-WT (grey) defined
1231 as the days after sowing (DAS) at which half of the first ear has emerged past the ligule. Upper and
1232 lower hinges represent the first and third quartiles (25th and 75th percentiles), the middle hinge
1233 represents the median value, yellow triangle represents mean value and black dots represent
1234 individual replicates (n = 5). (B) Mean *Fm'* of lines shown in (A) in LL with SEM bars (n = 24). (C) RAE
1235 where points below dashed line considered rhythmic (D) circadian period length (hours)and (E)
1236 amplitude for genotypes inplot (B). Box jitter plots as described above, note plotted points in (C-E)

correspond to those where data was successfully fitted by FFT-NLLS model in Biodare2. Significant differences ($p < 0.05$) calculated in R using Kruskal-Wallis test followed by post-hoc Dunn's test.

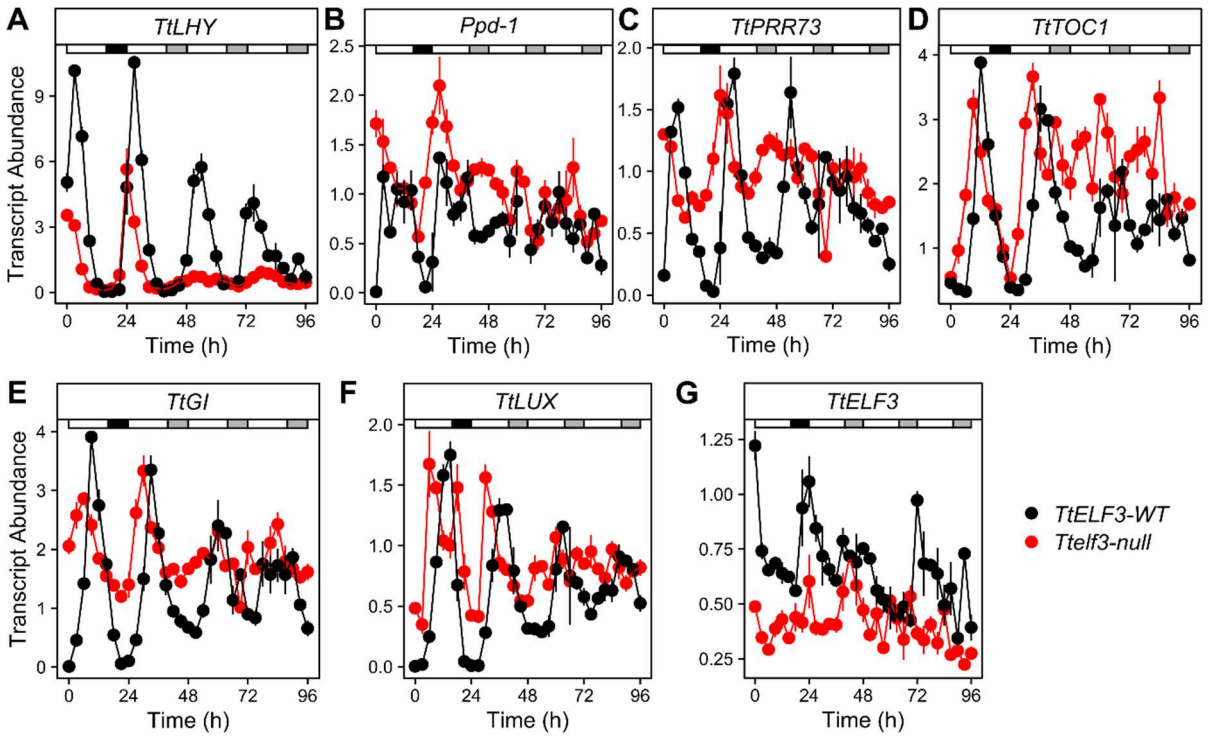

Figure 6. Abundance of wheat circadian clock transcripts in the *TtELF3-WT* and *ttelf3* lines in LD and LL.

(A-G) Mean abundance of circadian oscillator transcripts (n= 3 - 5) in *TtELF3*-WT (black) and *Ttelf3*-null (red) in a 24 h LD cycle in long day conditions (16 h light at 250 µmol m^{-2} s^{-1}, 20°C: 8 h dark 16°C, represented by horizontal grey bar) followed by constant light and temperature (20°C) from time 24 to 96 h. Transcript abundance (ΔΔCq) is relative to *TtRP15* and *TtRPT5A* (A) *TtLHY,* (B) *Ppd-1,* (C) *TtPRR73,* (D) *TtTOC1,* (E) *TtGI,* (F) *TtLUX* and (G) *TtELF3* . White bar represents light, black bar represents darkness and grey bar represents subjective night.

1274

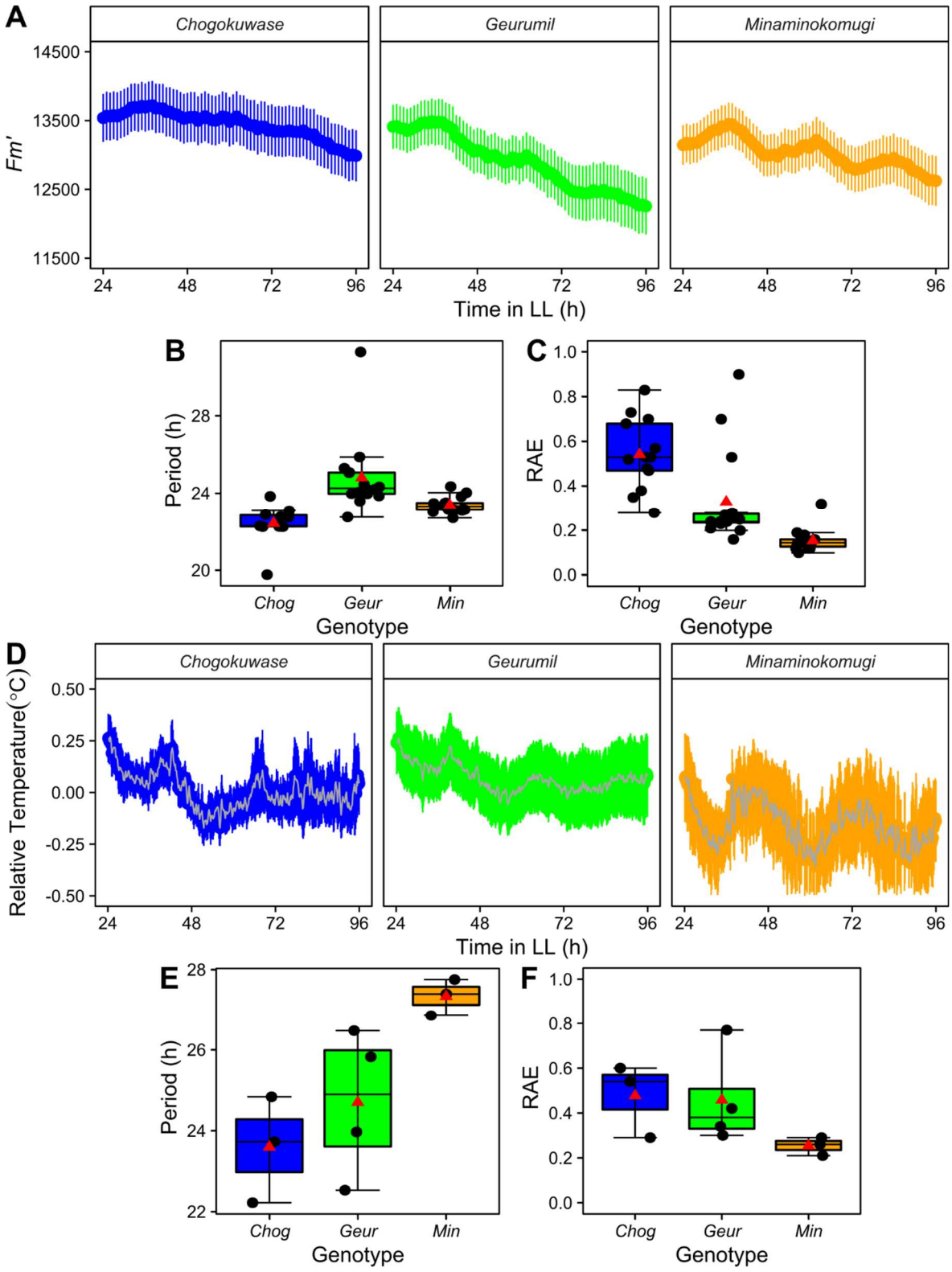

1275

1276 **Figure 7. Functional *LUX* is required for maintenance of robust circadian oscillations under LL**

1277 **conditions in hexaploid wheat.**

1278 (A) Mean $F_{m'}$ for Chogokuwase (blue), Geurumil (green) and Minaminokomugi (orange) in LL (n = 16)

1279 (B) Mean period and (C) RAE for (A) calculated using FFT-NLLS (Biodare2). Upper and lower hinges

represent the first and third quartiles (25th and 75th percentiles), the middle hinge represents the median value, red triangle represents mean value and black dots represent individual replicates. (D) Mean Chogokuwase, Geurumil and Minaminokomugi leaf temperature relative to background in LL (n = 4). (E) mean period and (F) RAE for plot (D). Error bars are SEM, for (D) every 20th point plotted for clarity.

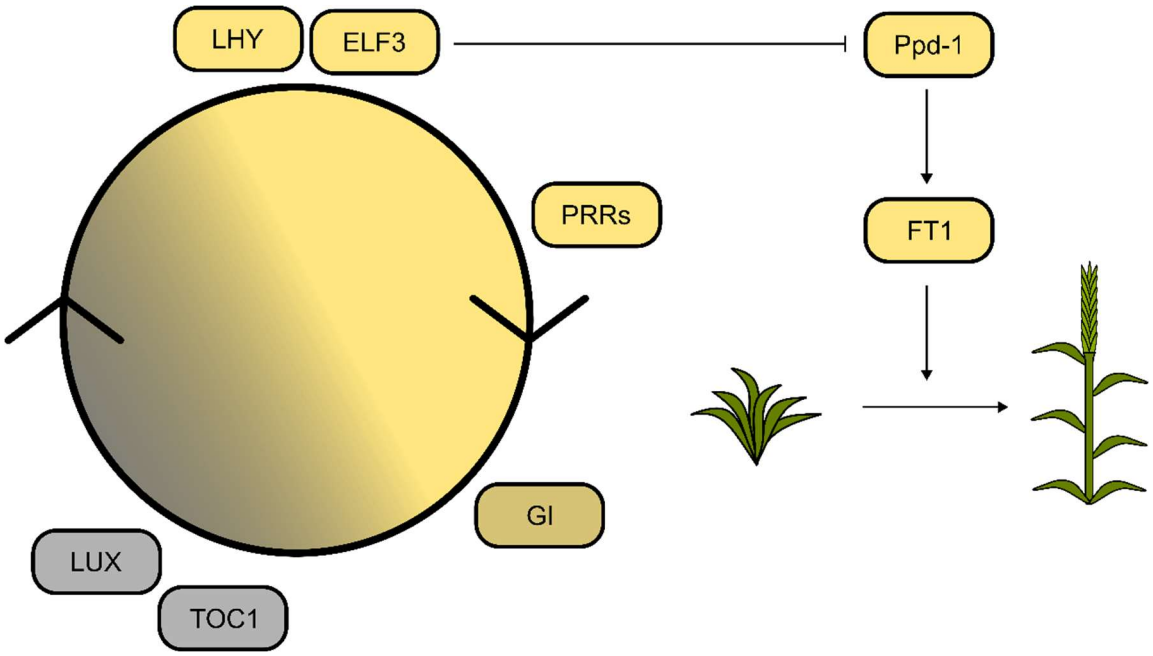

Figure 8: ELF3 functions in the circadian oscillator and regulates heading of wheat

Genes associated with the circadian oscillator are positioned and coloured relative to the time of day at which their transcript abundance is highest in LD. The progression of the circadian oscilaltor is indicated by the circle. Lines indicate potential regulatory links with outputs and other pathways. Pointed arrow heads represent activation and blunt arrowhead represents repression.

1327 **Table 1**: **Summary of circadian clock associated QTLs and their mapping positions.** Output from
1328 univariate QTL model for the NIAB 2013 and 2014 GS55 data. Gene (Mb) refers to the BLAST hit
1329 starting coordinate of the gene's cDNA against the IWGSCRefSeqv1.1. Dist (cM) refers to the markers
1330 genetic mapping distance in centiMorgan. Dist (Mb) refers to the BLAST hit starting coordinate of the
1331 marker sequence against the IWGSCRefSeqv1.1 LOGP is –log10(p) which corresponds to the overall
1332 significance of the QTLs as a measure of its strength. % var is the percentage of genetic variance
1333 contributed by QTL. Further description of methodology and column headers can be found in (Verbyla
1334 et al. 2014).

Circadian clock gene	Gene (Mb)	Chr	L. Marker	dist (cM)	dist (Mb)	R. Marker	dist (cM)	dist (Mb)	Year	LOGP	% var
TaELF3	685,646,575	1B	Ra_c109187_371	296.34	685,741,261	RAC875_c37075_283	297	687,715,336	2013	4.48	3.4
		1B	Ra_c109187_371	296.34	685,741,261	RAC875_c37075_284	297	687,715,336	2014	3.2	2
TaELF3	493,485,612	1D	Kukri_c29687_369	100.95	493,212,138	Kukri_rep_c69829_307	101.95	488,577,079	2014	2.32	4.1
Ppd-1	33,952,591	2D	Kukri_c27309_590	48.57	31,806,310	BS00064538_51	56.64	33,370,535	2013	20.04	17.2
		2D	Kukri_c27309_590	48.57	31,806,310	BS00064538_51	56.64	33,370,535	2014	43.92	30.2
TaZTL	625,638,942	7A	Kukri_c6676_172	207.62	610,934,248	Ku_c2990_1939	208.12	621,322,194	2013	2.87	2.6

1335
1336
1337
1338
1339
1340
1341
1342
1343
1344
1345
1346
1347

1348 **Table 2. 2013 and 2014 GS55 QTL summary for the *eps-B1 locus*.** Estimated parental haplotype
1349 effects on RIL BLUPs. Abbreviations as per (Verbyla *et al.* 2014): Dist (cM) refers to the markers
1350 genetic mapping distance in centiMorgans (cM). LOGP is –log10(p) and corresponds to the overall
1351 significance of the QTL as a measure of its strength. Founder Prob: probability QTL is from founder
1352 shown (p). Strength of associations can thus be reported at the overall or founder level. Size: Size of
1353 effect of each founder allele (days to GS55).
1354

QTL	Year	Founder	Size	Founder Prob	% var	LOGP	KASP (chr1B:685645813)
Eps-B1	2013	Alchemy	-0.555	0.054	3.4	4.48	A:A
		Brompton	0.317	0.123			G:G
		Claire	-0.076	0.415			A;A
		Hereward	0.623	0.008			G:G
		Rialto	0.331	0.118			G:G
		Robigus	-0.102	0.376			A:A
		Soissons	-0.683	0.003			A:A
		Xi-19	0.053	0.426			G:G
Eps-B1	2014	Alchemy	-0.448	0.196	2	3.2	A:A
		Brompton	0.395	0.178			G:G
		Claire	-0.442	0.202			A:A
		Hereward	0.591	0.072			G:G
		Rialto	0.39	0.182			G:G
		Robigus	-0.313	0.264			A:A
		Soissons	-1.085	0.002			A:A
		Xi-19	0.453	0.15			G:G

1355
1356
1357
1358
1359
1360
1361
1362
1363
1364
1365
1366

1367 **Table 3. 2012 and 2014 GS55 QTL summary for the *eEps-D1 locus*.** Estimated parental haplotype
1368 effects on RIL BLUPs. Abbreviations as per (Verbyla *et al.* 2014): Dist (cM) refers to the markers
1369 genetic mapping distance in centiMorgans (cM). LOGP is –log10(p) and corresponds to the overall
1370 significance of the QTL as a measure of its strength. Founder Prob: probability QTL is from founder
1371 shown (p). Strength of associations can thus be reported at the overall or founder level. Size: Size of
1372 effect of each founder allele (days to GS55).
1373

QTL	Year	Founder	Size	Founder Prob	% var	LOGP	PCR (Figureure 3D)
Eps-D1	2012	Alchemy	0.552	0.254	0.9	0.56	1097bp
		Brompton	0.105	0.446			1097bp
		Claire	-0.11	0.447			1097bp
		Hereward	0.021	0.49			1097bp
		Rialto	-0.044	0.477			1097bp
		Robigus	0.003	0.498			1097bp
		Soissons	0.734	0.134			1097bp
		Xi-19	-1.261	0.015			776bp
Eps-D1	2014	Alchemy	-0.058	0.472	4.1	2.32	1097bp
		Brompton	0.869	0.104			1097bp
		Claire	-1.412	0.051			1097bp
		Hereward	-0.582	0.252			1097bp
		Rialto	-0.071	0.457			1097bp
		Robigus	-0.265	0.38			1097bp
		Soissons	1.244	0.013			1097bp
		Xi-19	-0.79	0.053			776bp

1374
1375
1376
1377
1378
1379
1380

1381 **Table 4: Wheat lines used in this study.** GRU refers to the germplasm resource unit at the John Innes

1382 Centre, Norwich.

Species	Cultivar	Genotype	Reference
Ae. speltoides			GRU 2140023
T. aestivum	Alchemy		(Mackay *et al.* 2014)
T. aestivum	Brompton		(Mackay *et al.* 2014)
T. aestivum	Claire		(Mackay *et al.* 2014)
T. aestivum	Hereward		(Mackay *et al.* 2014)
T. aestivum	Rialto		(Mackay *et al.* 2014)
T. aestivum	Robigus		(Mackay *et al.* 2014)
T. aestivum	Soissons		(Mackay *et al.* 2014)
T. aestivum	Xi-19		(Mackay *et al.* 2014)
T. aestivum	Cadenza		GRU WBCDB0013-PG1
T. aestivum	Jagger		GRU PANG0006
T. aestivum	Spark		GRU WBCDB0052
T. aestivum	Chinese Spring		
T. aestivum	Chogokuwase		(Mizuno *et al.* 2016)
T. aestivum	Minaminokomugi		(Mizuno *et al.* 2016)
T. aestivum	Geurumil		(Mizuno *et al.* 2016)
T. aestivum	Axona		GRU W3580
T. aestivum	Cordiale		GRU W10003
T. aestivum	Maris Fundin		GRU W1357
T. aestivum	Tonic		GRU W3572
T. monococcum			GRU T1040057
T. sphaerococcum			GRU 1210007
T. timopheevii			GRU 116002
T. turgidum	Kronos	*Ttelf3*-null line	(Alvarez *et al.* 2016)
T. turgidum	Kronos	*TtELF3*-WT	(Alvarez *et al.* 2016)
T. turgidum	Kronos	*Ttelf3*-Anull	In house
T. turgidum	Kronos	*Ttelf3*-Bnull	In house

1383

1384

1385

1386

1387

1388

1389

1390

1391 **Table 5: Primers used in this study**

Gene	Sequence 5'-3'
TtCCA1	F: CCTGGAATTGGAGATGGAGA
	R: TGAGCATGGCTTCTGATTTG
TtELF3	F: TCTCCAGATGATGTTGTCGGT
	R: CTCGAACACTTGGACAGCAAA
TtGI	F: GGTAGGTGATAGACGGCACTT
	R: GTGCTACAGATGGGATGCTTG
TtFT1	F: TGAGGACCTTCTACACACTCG
	R: ACCGGGGATATCTGTCACAAG
TtLUX	F: ACAAGCGGTTCGTGGAGG
	R: CCTGCATCCGCTTGACGTA
TtPpd-1	F: CCTGTGGACTGTCGATCTCAA
	R: CAAGGGATGGCAGCGATAATG
TtPRR73	F: TCCCGAAGTTCCTCTCTTTCC
	R: AGCGGTAGTGGCAATGACA
TtTOC1	F: GGCATGGCACTTCATTCAGTT
	R: GCACATTCATACCAGCAGGAC
TtRP15	F: GCACACGTGCTTTGCAGATAAG
	R: GCCCTCAAGCTCAACCATAACT
TtRPT5A	F: GCTGGCTCGTTCAACTGATG
	R: GGACCAAGCGTTCTGATTACTC
TaELF3-D1	F: CAACGGCGCTTCTAATCTG
	R: AAACCCGCTGCTGACTGTATA

1392